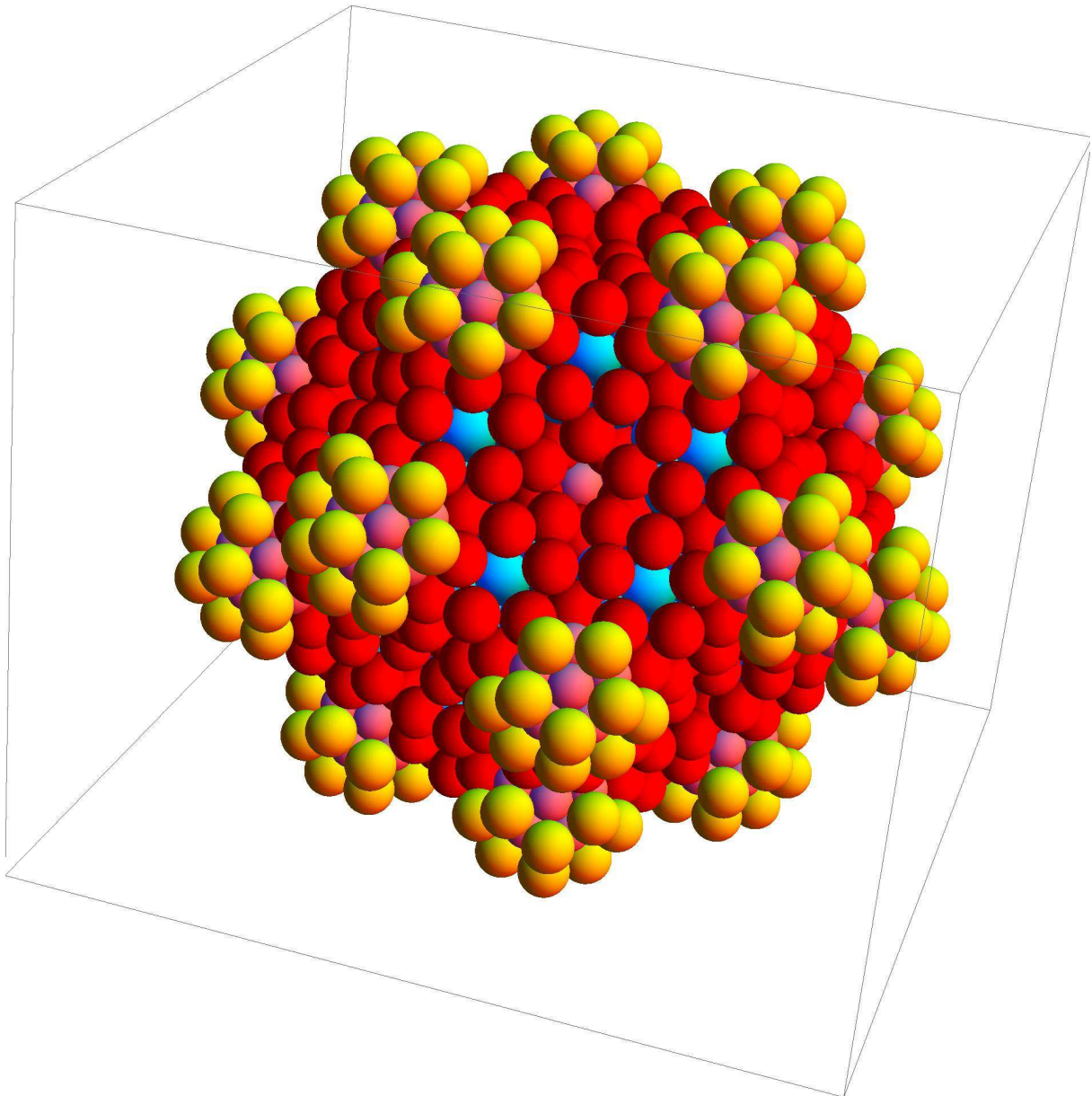


Hartwig Schlüter

**Models of the Atomic Structure of  
Approximants and Related Quasicrystals**



CIP-Kurztitelaufnahme der Deutschen Bibliothek  
Schlüter, Hartwig:  
Models of the Atomic Structure of Approximants  
and Related Quasicrystals / Hartwig Schlüter  
SCHLÜTER CONSULT Dr. Hartwig Schlüter, Göttingen 2011

ISBN 978-3-9814911-0-4 SCHLÜTER CONSULT Dr. Hartwig Schlüter, Göttingen

Copyright © 2011 SCHLÜTER CONSULT Dr. Hartwig Schlüter. All rights reserved. Only for nonprofit educational purposes you may not need to ask permission to use parts of this file, but you still must *cite* these images and/or the used text!

Cover Design: Hartwig Schlüter and Harald Schlüter

SCHLÜTER CONSULT  
Dr. Hartwig Schlüter  
Maschmühlenweg 8-10  
D-37073 Göttingen  
Germany  
[www.schlueter-consult.de](http://www.schlueter-consult.de)

Convictions are prisons.

Nitzsche

## **Contents**

	Preface	
	Abbreviations	
1	Introduction	1
2	Self-Similarity of Sphere/Atom Clusters with Icosahedral Symmetry	2
3	A Model of the Atomic Structure of an Icosahedral Approximant	10
3.1	A Model of the Atomic Structure of Icosahedral Quasicrystals	20
4	Models of the Atomic Structure of Decagonal Approximants	26
4.1	Models of the Atomic Structure of Decagonal Quasicrystals	32
	Appendix: A Nomenclature of Clusters	36
	References	38

## Preface

This publication is a short version of parts of the book entitled “*Quasikristalle - selbstähnliche Atomcluster “am Rande des Chaos“*“ [2], which means “Quasicrystals - Self-Similar Atom Clusters “on the Brink of Chaos““.

The suggestion to show stereo pictures of the sphere models came from Dr. Eckart Baum and during the realisation of the sphere models and computer illustrations, great support was given by Mr. Reinhard Bögge, Mrs. Petra Dörfler, Mr. Erich Schlüter sen., Mrs. Else Schlüter and Dr. Harald Schlüter. For their valuable suggestions and active support I am very grateful.

The models of the atomic structure of quasicrystals described here were presented in 1999 at the spring meeting of the DPG in Münster, at the fall meeting of the MRS in Boston in 2000 and at the spring meeting of the DPG in Hamburg in 2001.

A 3D animation of some clusters described here will be performed with the software “Mathematica®” and presented in a separate publication - “*A Cookbook for Sphere Clusters on the Base of “Mathematica®”*”, Volume 1, (Hartwig Schlüter and Harald Schlüter, SCHLÜTER CONSULT, Göttingen, 2011).

Göttingen, December 2011

Hartwig Schlüter

Wolfram Mathematica® is a registered trademark of Wolfram Research, Inc.

## Abbreviations

ik-cluster	cluster with icosahedral symmetry (Mackay cluster and Bergman cluster)
cluster{m}	cluster of the m <sup>th</sup> generation
cluster{m'}layer{m}	cluster{m'} layer of the m <sup>th</sup> generation
cluster{m'}5f-layer{m}	cluster{m'}layer{m} with one common 5-fold symmetry axis
column{m}	ik-cluster-layer column of the m <sup>th</sup> generation
columns{m;m'}	ik-cluster-layer columns of the m <sup>th</sup> and m' <sup>th</sup> generation
5f-column{m}	column{m} with one 5-fold symmetry axis
3f-axis	axis with 3 fold symmetry
5f-symmetrie	5 fold symmetry
i-quasicrystal	icosahedral quasicrystal
d-quasicrystal	decagonal quasicrystal
HRTEM	high resolution transmission electron microscope

## 1 Introduction

*You may say I'm a dreamer  
but I'm not the only one*  
John Lennon (Imagine)

*- I hope so!*  
The Author

By the discovery of quasicrystals in 1982 Dan Shechtman introduced us to an exciting new area of solid state physics and chemistry [1].

Beside the complex structure of quasicrystals, another striking feature is their extraordinary hardness. With a knowledge of applicable structure models, it may be possible to “design“ new quasicrystalline alloys with desired material properties in combination with this high degree of hardness.

In Section 2 a general overview about self-similar sphere clusters with icosahedral symmetry is given and in Section 3 and 4 special sphere clusters are presented as prototype structures for icosahedral and decagonal approximants, respectively. An interesting property of the prototype structures is the high percentage (about 40%) of coincidence places for spheres/atoms; this means that spheres/atoms belong to two or three nearest neighbor clusters equally. The following assumption gives some credence to the validity of the structure models described in the following sections. In an alloy that forms i-quasicrystals or d-quasicrystals at the solidification front, potential cluster positions with the most existing coincidence atom positions that are shared with already solidified atom clusters may occur with a higher probability than other potential atom clusters with less coincidence places.

In this publication quasicrystals will be described as approximants – as cluster crystals - with phasons and/or point defects like A-atoms on places for B-atoms and vice versa, vacancies, sphere/atom positions with an overlap. The meaning of the expression “phason“ here goes beyond its use in the scientific literature; see Section 3.1 and 4.1.

The prototype structures allow the simulation of the growth of approximants and quasicrystals with cellular automata [2]. Under “en.wikipedia.org” “cellular automata” access is given to several cellular automata “in action”, e.g. “Game of Life” from John Conway.

A nomenclature for clusters has been created in order to have a simple characterisation for clusters [2][3]. A brief outline of the nomenclature of clusters is given in the appendix.

## 2 Self-Similarity of Sphere/Atom Clusters with Icosahedral Symmetry

*Big fleas have little fleas upon their backs  
to bite them  
and little fleas have lesser fleas, and so ad  
infinitum*

Jonathan Swift

In recent years, self-similar systems have become a favorite field of research for scientists and meanwhile a lot of different self-similar systems have been described and published [4][5][6]; reference [6] also contains very good introduction to cellular automata. Spheres can be put together to form many different types of self-similar clusters with icosahedral symmetry. Here some examples are described in order to demonstrate the construction principles. ik-clusters are of interest in relation to the search for appropriate structure models for quasicrystals [2].

Self-similar clusters are always discrete self-similar clusters.

**Figure 1** shows one sphere and three Mackay clusters in the first generation (Mackay clusters{1}) with different numbers of shells; this type of cluster with icosahedral symmetry (ik-cluster{1}) was first described by Mackay [7], it has  $n$  shells ( $1 < n < \infty$ ). One sphere is in the center (first shell; per definition), 12 spheres in the second shell, 42 spheres in the third shell, 72 spheres in the fourth shell etc. Another type of ik-cluster{1} is depicted in **Figure 2**. This Bergman cluster{1} also can have  $n$  shells ( $1 \leq n < \infty$ ). In both types of ik-clusters{1} 20 tetrahedrons with one 3-fold symmetry axis each can be found. Examples of these tetrahedrons are depicted in **Figure 3**. Neighbor tetrahedrons from the Mackay clusters{1} in **Figure 1** have coincidence places for spheres on the 5-fold axes of the Mackay clusters{1} (a blue sphere and the green spheres) and on the planes between two 5-fold axes (red spheres). This is not the case for the Bergman clusters{1} in **Figure 2**, but these Bergman clusters{1} have a hollow space in the center and additional spheres on the 5-fold axes; the orange spheres in **Figure 2**. In the incomplete outer shell of the Bergman clusters{1} in **Figure 2** only the positions on the 5-fold axes (orange spheres) are occupied. Later in this publication, when ik-clusters{2} are discussed, it will be shown that the first shell of this Bergman-type cluster{m} ( $m > 1$ ) has no ik-clusters{m-1} on the 5-fold axes. The hollow space in the center of Bergman clusters{1} can be filled e.g. with a Mackay cluster{1} of 13 smaller spheres – the diameter is about 80 % of the diameter of the spheres of the outer shell. An example is shown in **Figure 4**.

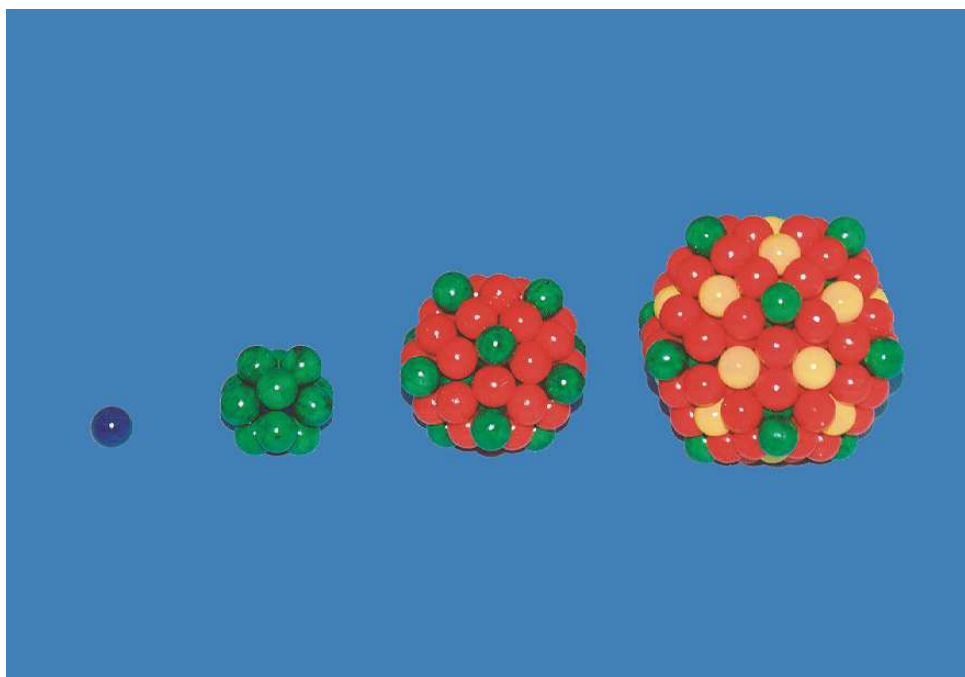


Figure 1: A single blue sphere and three Mackay clusters  $\{1\}$  with different numbers of shells.

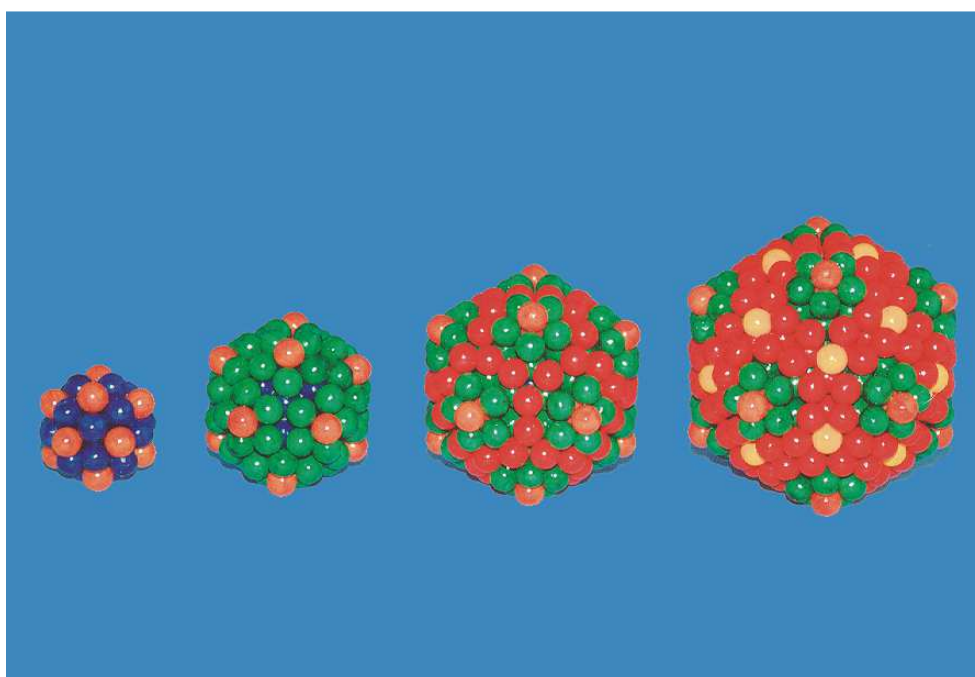


Figure 2: Four Bergman clusters  $\{1\}$  with different numbers of shells. The outer shell of the  $ik$ -clusters  $\{1\}$  is incomplete; only the positions on the 5-fold axes are occupied.

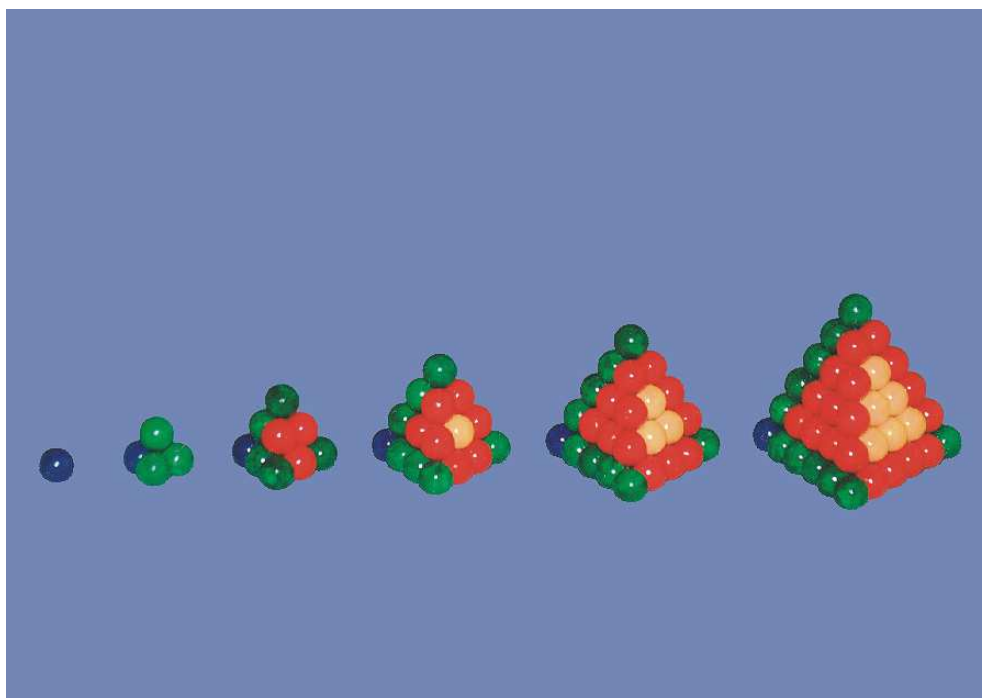


Figure 3: A single blue sphere and five tetrahedrons with different numbers of layers of spheres.

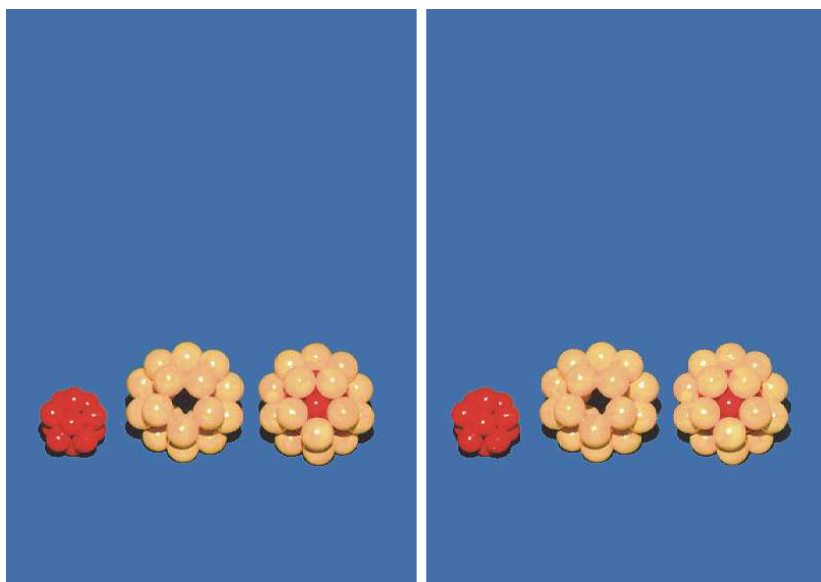


Figure 4: An example of how to fill the hollow space in the center of a Bergman cluster{1} with a Mackay cluster{1} of smaller spheres.

**For the 3D-view of the stereo pictures, the width of the page – also on the screen – should be in the range of 18 cm to 20 cm.**

In Reference [3] a general overview is given about the ways in which spheres can be put together in order to form ik-clusters{1}, and how the ik-clusters{1} can be used instead of spheres as building blocks in order to generate ik-clusters{2}, and how ik-clusters{2} can be used to form ik-clusters{3} etc. In these ik-clusters{m}, nearest neighbor ik-clusters{m-1} from nearest neighbor shells have a common 5-fold symmetry axis and nearest neighbor ik-clusters{m-1} from the same shell have a common 2-fold symmetry axis. All ik-clusters of all generations can have the same orientation of the symmetry axes.

If the building principle of the building blocks of an ik-cluster{m} ( $m \geq 2$ ) is the same for all ik-cluster generations, then this is an ideal self-similar ik-cluster{m} [3]. **Figure 5** shows a Mackay cluster{1}, an ideal self-similar Mackay-type cluster{2} and an ideal self-similar Mackay-type cluster{3}. All ik-clusters consist of 12 building blocks in every ik-cluster generation and the building principle is the same for all generations. A stereo image of the Mackay-type clusters{3} of **Figure 5** is shown in **Figure 6**.

If the building principle of the building blocks of an ik-cluster{m} ( $m \geq 2$ ) is only in part the same for all ik-cluster generations, then this is a partially self-similar ik-cluster{m} [3]. Two examples are depicted on the left side of **Figure 7 and 8**.

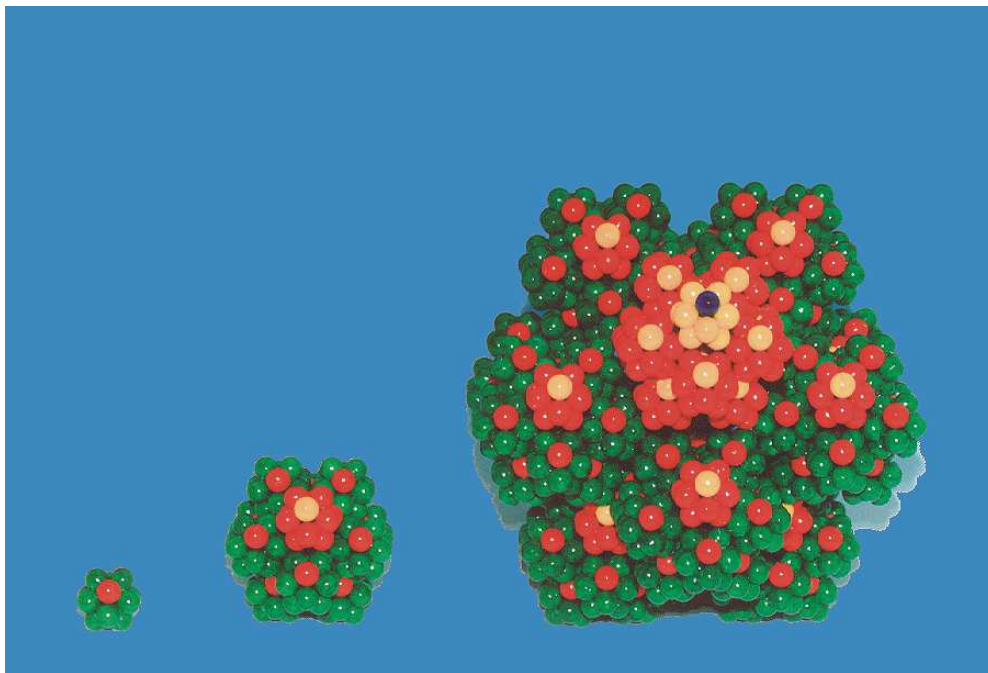


Figure 5: An Mackay cluster{1}, an ideal self-similar Mackay-type cluster{2} and an ideal self-similar Mackay-type cluster{3}.

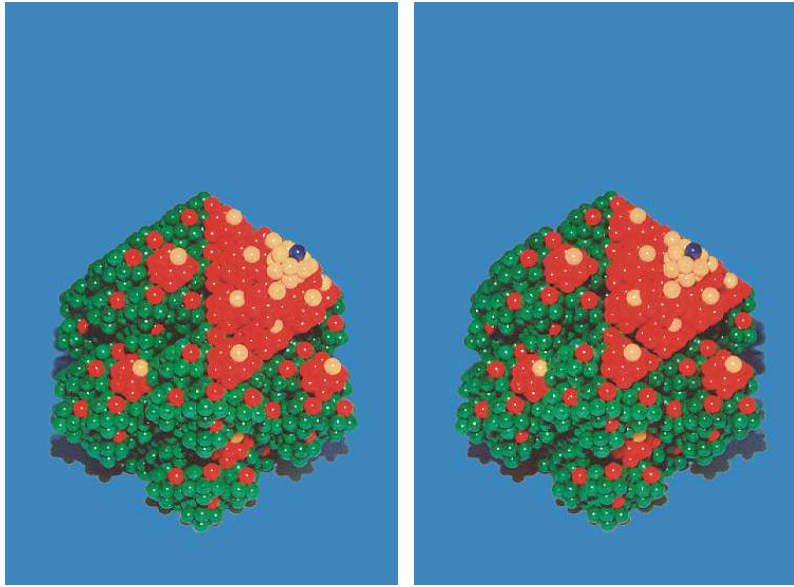


Figure 6: Stereo image of the ideal self-similar Mackay-type cluster{3} of Fig. 5.

The partially self-similar Bergman-type cluster{2} in **Figure 7** has the same construction principle as the Bergman cluster{1} on its right side, but the construction principle of the building blocks of the ik-cluster{2} is slightly different to its own construction principle. In this image it can be seen that the first shell of this Bergman-type cluster{2} has no building blocks on the 5-fold axes. The orange Bergman clusters{1} have a common 5-fold axis with the blue nearest neighbor Bergman clusters{1} - the blue ik-clusters{1} belong to the first shell of the ik-cluster{2} and the orange ik-clusters{1} to the second shell. The red spheres are put between nearest neighbor ik-clusters{1} from nearest neighbor shells in order to prevent an overlapping of nearest neighbor ik-clusters{1} from the same shell.

The Mackay cluster{1} on the right side of **Figure 8** has the same building principle as the partly self-similar Mackay-type cluster{2} on the left side of this figure. But the ik-cluster{2} has a different building principle than its building blocks – the Bergman clusters{1}. **Figure 9** illustrates the shell by shell growth of the two Mackay-type clusters of **Figure 8**. The blue spheres are put between nearest neighbor ik-clusters{1} from nearest neighbor shells in order to prevent their overlapping. The yellow ik-clusters{1} from the fourth shell of the ik-cluster{2} in **Figure 8** form together an ik-cluster{2} that is self-similar in relation to themselves.

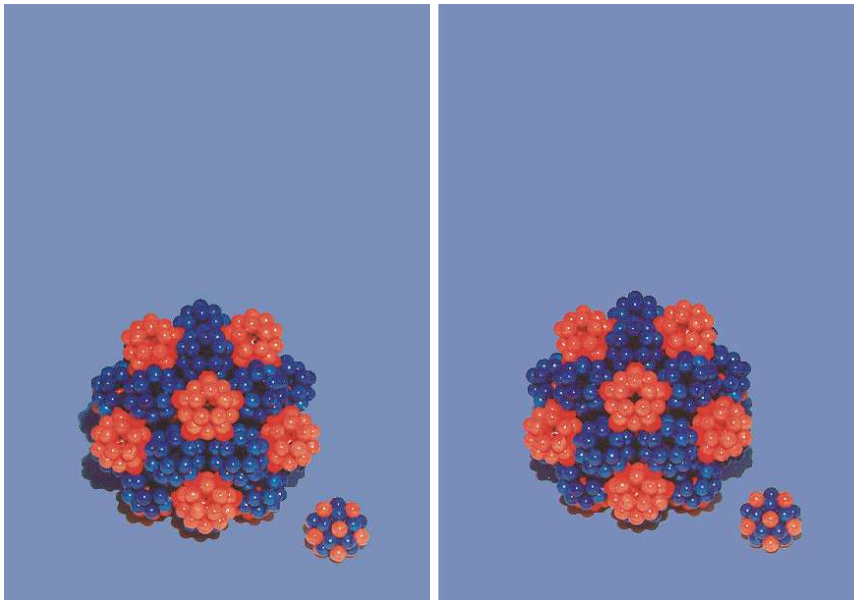


Figure 7: The partially self-similar Bergman-type cluster{2} on the left side has the same construction principle as the Bergman cluster{1} on the right side.

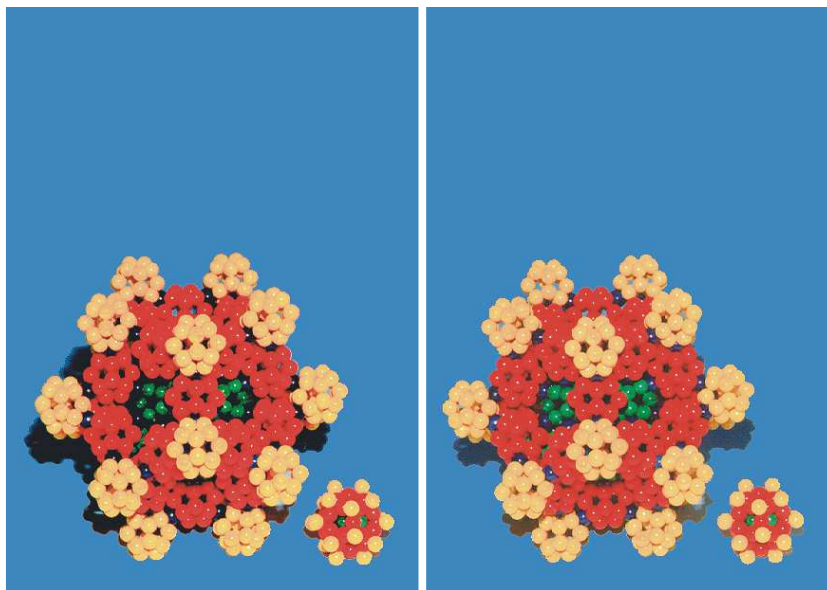


Figure 8: The partially self-similar Mackay-type cluster{2} on the left side has the same construction principle as the Mackay cluster{1} on the right side.

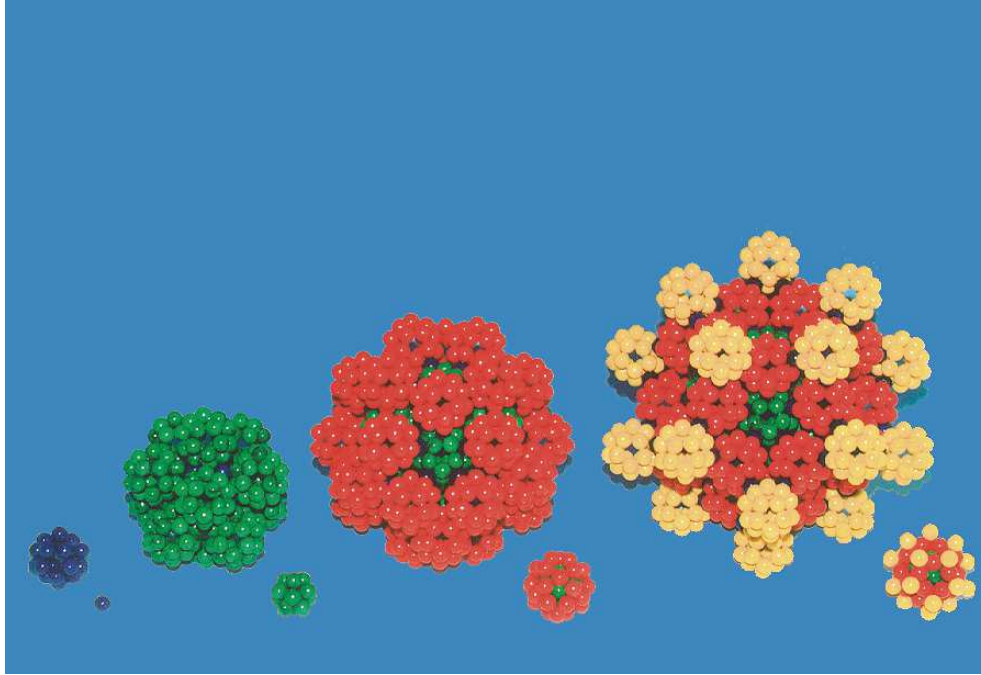


Figure 9: This Figure illustrates the shell by shell growth of Mackay-type cluster{2} and the analogous Mackay cluster{1}.

If building blocks in analogous positions are removed from each ik-cluster that belongs to an ideal self-similar ik-cluster{m} ( $m \rightarrow \infty$ ), then the voids also form an ideal self-similar “void-cluster“. For example, from all ik-clusters of an ik-cluster{10} with  $n = 20$  shells and the same building principle in all generations, the building blocks on their 5-fold and/or 3-fold and/or 2-fold axes, which are in shells with an unpaired and/or paired index are removed; this kind of ik-cluster resembles a “Menger-Sponge“; see for e.g. reference [6].

It is possible to remove and/or add building blocks on analogous or not analogous positions in ik-clusters of some or all generations. In different ways an ideal self-similar ik-cluster{m} can be transformed into a partially self-similar ik-cluster or step by step into a not self-similar ik-cluster by removing different building blocks from all ik-clusters of all generations.

For ik-clusters{m} it is possible

- that different ik-clusters{m-1} can be put in the same shell of an ik-cluster{m},
- that all/some building blocks of an ik-cluster{m} are different and these building blocks can also belong to different generations  $\{m'\} \leq \{m-1\}$
- that building blocks of shells with an unpaired index can differ in size and building principle from the building blocks of shells with a paired index (see Section 3),
- that nearest neighbor ik-clusters{m-1} from the same shell and/or from the nearest neighbor shell can have coincidence building blocks (see Section 3), nearest neighbor ik-clusters{m-1} from the same shell and/or from the nearest neighbor shell can touch each other (overlap of less than 1%), nearest neighbour ik-clusters{m-1} can have an overlap and nearest neighbour ik-clusters{m-1} can have no contact or overlap.

- that the interstitial space between building blocks is filled by spheres or ik-clusters  $\{m'\}$ ,
- that the (filled) interstitial space between building blocks is seen as a cluster,
- that ik-clusters  $\{m\}$  form cluster layers and these cluster layers can form cluster columns (see Section 4 and 4.1),
- that the order within ik-clusters  $\{m\}$  can be degraded step by step or continuously.
- that the spheres can be replaced by “whatever”
- that the size of the building blocks can increase or decrease from one shell to another [3],
- to describe unit cells of ik-clusters  $\{m \rightarrow \infty\}$  with a number  $n'$  of atoms ( $n' \rightarrow \infty$ ); e.g. the building principle of the T'1-cluster $\{2\}$  and T'2-cluster $\{2\}$  (see Section 3) is repeated for the following  $m' \leq m-1$  cluster generations and the T\*1-cluster $\{m\}$  or the T\*2-cluster $\{m\}$  has e.g. 10 cluster shells – contains 20 single crystals with 10 cluster layers each.
- etc. [3].

Other types of self-similar ik-clusters  $\{m\}$ :

- Self-similar ik-clusters with  $n$  shells can be constructed by taking  $n$  shells of pearls/clusters with the same building principle and the same orientation but of different size, and a smaller shell is always put into the next bigger shell.

Now it is the task to find out of all possible sphere clusters the suitable models for i-quasicrystals and d-quasicrystals.

### 3 A Model of the Atomic Structure of an Icosahedral Approximant

*Observation always involves theory*

Edwin Hubble

A prototype approximant structure will be described in this section and discussed in Section 3.1 in relation to the structure of related icosahedral quasicrystals (i-quasicrystals). A very detailed description and discussion of this model is given in reference [2].

Since transmission electron microscope investigations of an AlCuFe alloy reported by Audier and Guyot [8] gave evidence of a reversible structural transformation between an i-quasicrystalline phase and a crystalline rhombohedral approximant phase, it might be useful to derive structure models for i-quasicrystals from suitable rhombohedral approximant structures, containing ik-clusters.

The proposed prototype approximant structure can be found in each of the 20 single-crystals of an ik-cluster{3}. A striking feature of this structure is the high number of coincidence places for spheres that are shared by nearest neighbor ik-clusters{1} from the same shell and from nearest neighbor shells. About 40 % of the sphere positions belong to two or three ik-clusters{1} equally. The clusters of all generations have icosahedral symmetry and also have the same orientation of the symmetry axes.

Two different types of ik-clusters{1} are used to build two different types of ik-clusters{2}. **Figure 10** shows on the left side a model of the third shell of a T1-cluster{1} (Mackay) and on the right side a model of the T2-cluster{1} (Bergman with Mackay inside (red)) – T stands for “type”. Nearest neighbor spheres in the same shell of an ik-cluster{1} must touch each other. The overlap between nearest neighbor spheres from nearest neighbor shells is allowed or modified spheres like the one shown in **Figure 11** can be used.

A T1-cluster{1} has one sphere in the center (first shell). 12 spheres are on the six 5-fold symmetry axes of the T1-cluster{1} (second shell) and 30 spheres are located on the 15 2-fold symmetry axes of the T1-cluster{1} (third shell); all spheres have the same size. This type of ik-cluster{1} is very similar to a “Mackay icosahedron” [7].

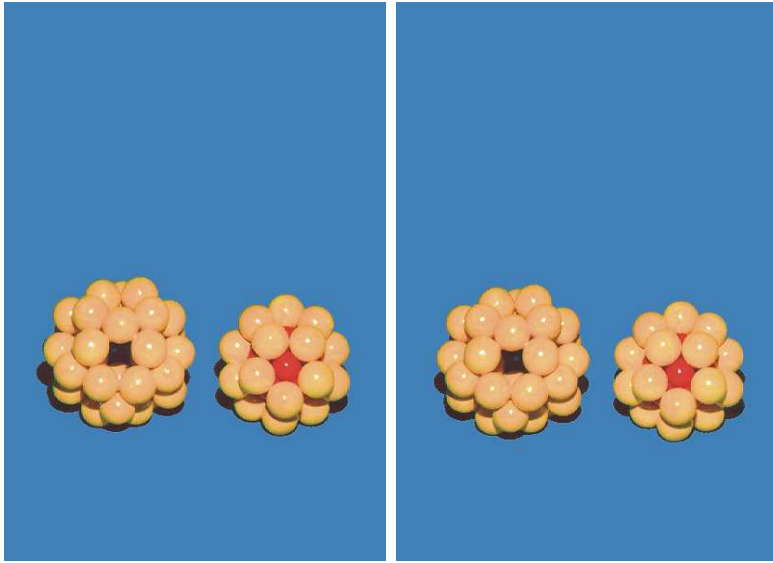


Figure 10: A model of the third shell of a T1-cluster{1} (Mackay) on the left side and a model of the T2-cluster{1} (Bergman; Mackay inside (red)) on the right side.

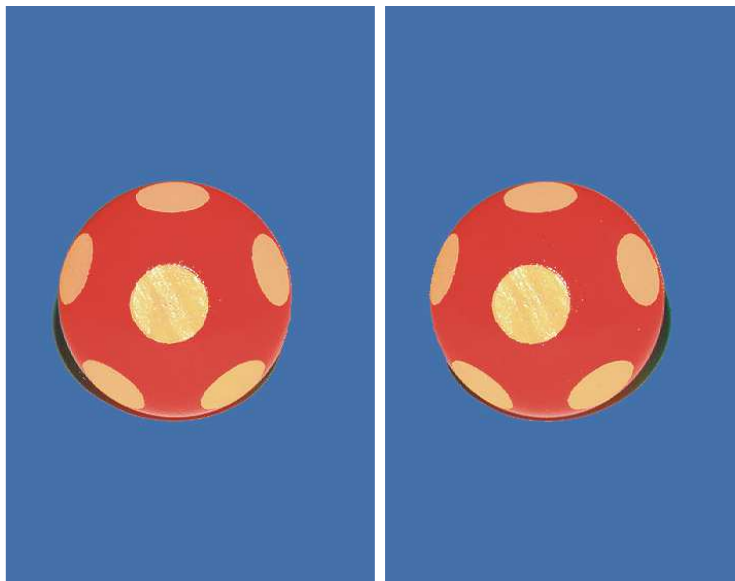


Figure 11: A sphere, chopped perpendicular to six 5-fold axes; see text.

The T2-cluster{1} has 20 spheres of the same size as the spheres in the T1-cluster{1}. The centers of the spheres are in the corners of a virtual pentagon dodecahedron. Inside of this shell there are 12 spheres (the red ones in **Figure 10**) which have a diameter of 82.4 % of the other spheres. These smaller spheres touch the larger nearest neighbor spheres of the T2-cluster{1}. In the center of a T2-cluster{1} is one of the smaller spheres, which overlaps with its 12 nearest neighbor spheres.

A model of the T'1-cluster{2} is depicted on the left side of **Figure 12**, together with an analogous ik-cluster{1} on the right side. And **Figure 13** shows a model of the T'2-cluster{2} on the left side, again together with an analogous ik-cluster{1} on the right side. In these ik-clusters, analogous shells are marked by the same color. The shell by shell growth of a model of the T'1-cluster{2} and of an analogous ik-cluster{1} is illustrated in **Figure 14** and for a model of the T'2-cluster{2} and an analogous ik-cluster{1} in **Figure 15**. The spheres from the outer shell of T2-clusters{1} which are not on coincidence places with spheres of a T1-cluster{1} in the shell below as well as the spheres from the inner shells of the T1-cluster{1} are removed from the models of the T'1- and T'2-cluster{2}, in order to facilitate the model construction. The inner 13 spheres of the T1-cluster{1} have been removed as well.

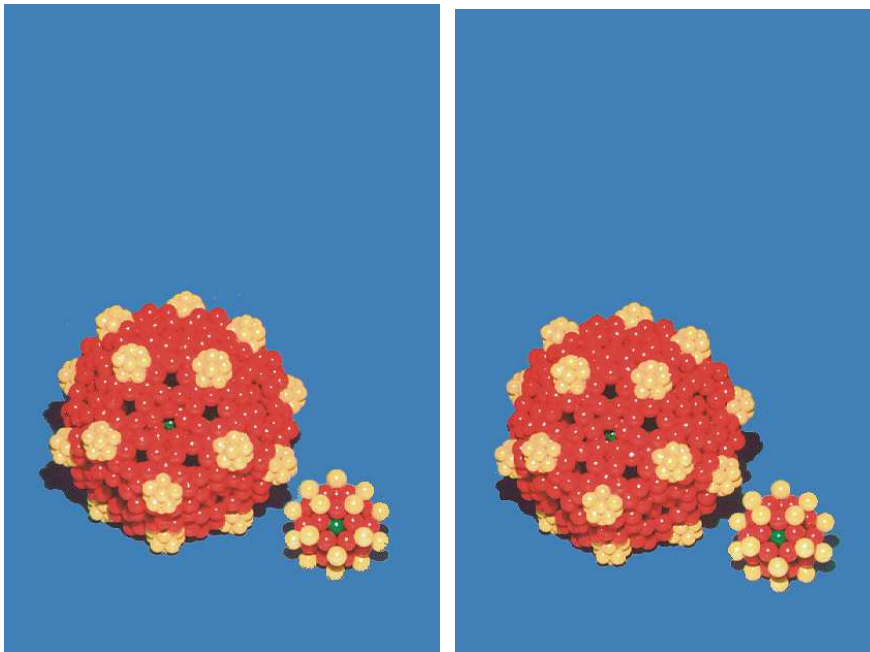


Figure 12: A model of the T'1-cluster{2} on the left side. The positions occupied with T1- and T2-clusters{1} are analogous to the positions of the spheres of the ik-cluster{1} on the right side.

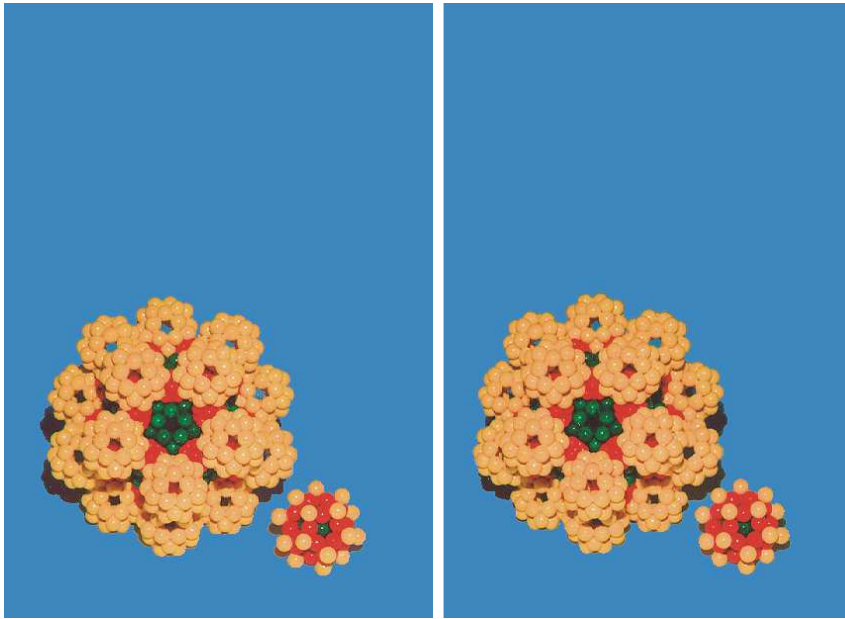


Figure 13: A model of the  $T'2\text{-cluster}\{2\}$  on the left side. The positions occupied with  $T1$ - and  $T2\text{-clusters}\{1\}$  are analogous to the positions of the spheres of the  $ik\text{-cluster}\{1\}$  on the right side.

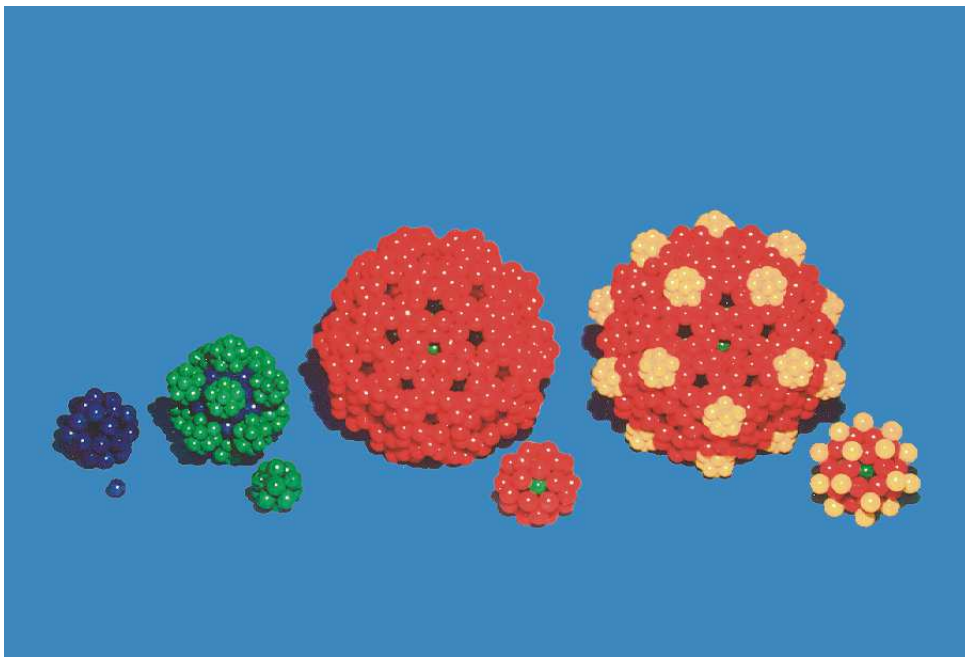


Figure 14: The shell by shell growth of a model of the  $T'1\text{-cluster}\{2\}$  and of an analogous  $ik\text{-cluster}\{1\}$ ; see also Fig. 12.

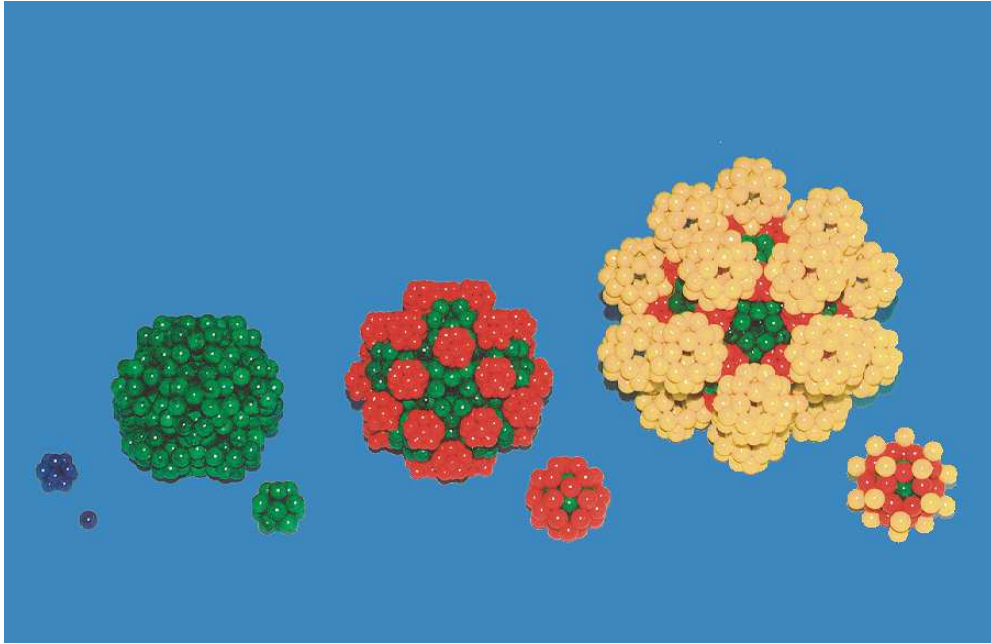


Figure 15: The shell by shell growth of a model of the  $T'2\text{-cluster}\{2\}$  and of an analogous  $ik\text{-cluster}\{1\}$ ; see also Fig. 13.

A  $T'1\text{-cluster}\{2\}$  as well as a  $T'2\text{-cluster}\{2\}$  has one  $ik\text{-cluster}\{1\}$  in the center (first shell), 12  $ik\text{-clusters}\{1\}$  on the 6 5-fold symmetry axes (second shell) and 30  $ik\text{-clusters}\{1\}$  on the 15 2-fold symmetry axes (third shell); the positions on the 5-fold axes are not occupied in this shell. In the incomplete fourth shell only 20  $ik\text{-clusters}\{1\}$  are located on the 10 3-fold symmetry axes of the  $ik\text{-cluster}\{2\}$  – these 20  $ik\text{-clusters}\{1\}$  are Bergman-type cluster $\{2\}$ . Nearest neighbor  $ik\text{-clusters}\{1\}$  in the same shell have a common 2-fold axis and nearest neighbor  $ik\text{-clusters}\{1\}$  from nearest neighbor shells have a common 5-fold axis. A  $T'1\text{-cluster}\{2\}$  has  $T1\text{-clusters}\{1\}$  in the first and in the third shell and  $T2\text{-clusters}\{1\}$  in the second and fourth shell. For a  $T'2\text{-cluster}\{2\}$  the packing of the two different types of  $ik\text{-clusters}\{1\}$  is vice versa.

Nearest neighbor  $ik\text{-clusters}\{1\}$  from nearest neighbor shells have 5 coincidence places for spheres; this is illustrated in **Figure 16**. An overlap is allowed for nearest neighbor spheres from the second shell of nearest neighbor  $ik\text{-clusters}\{1\}$  with a common 5-fold symmetry axis. Nearest neighbor  $T1\text{-clusters}\{1\}$  which are in the second or third shell of an  $ik\text{-cluster}\{2\}$  have 4 coincidence spheres (see **Figure 17**). In the third shell of  $T1\text{-clusters}\{1\}$  the nearest neighbor sphere to these four coincidence places has to be removed. The nearest neighbor  $T2\text{-clusters}\{1\}$  that are in the second or third shell of an  $ik\text{-cluster}\{2\}$  have 2 coincidence spheres (see **Figure 18**).

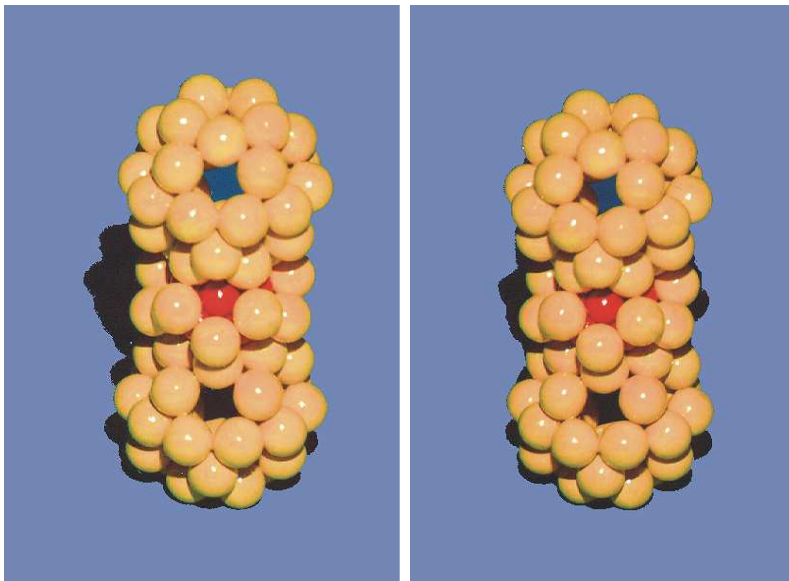


Figure 16: Each of two third shells of T1-clusters{1} shares a common 5-fold axis and five coincidence places for spheres with the central T2-cluster{1}. All three clusters have the same orientation of the symmetry axes.

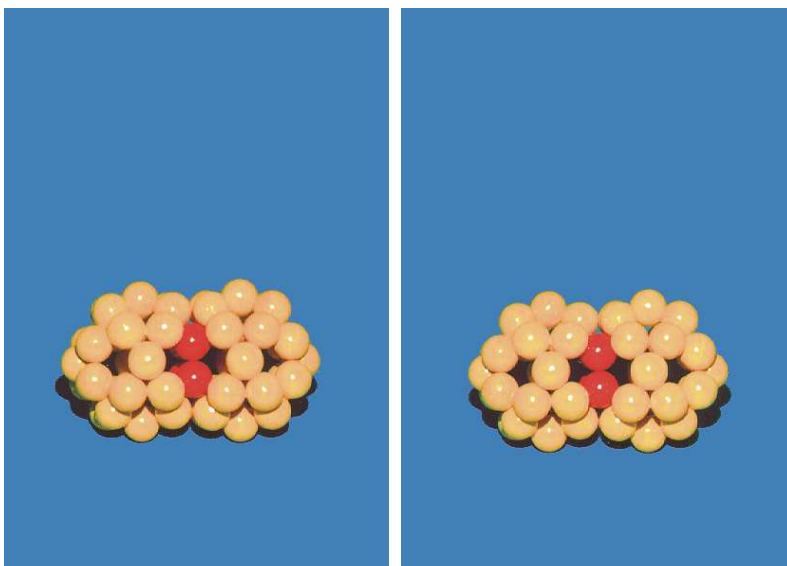


Figure 17: Two third shells of T1-clusters{1} with a common 2-fold axis and four coincidence spheres (red).

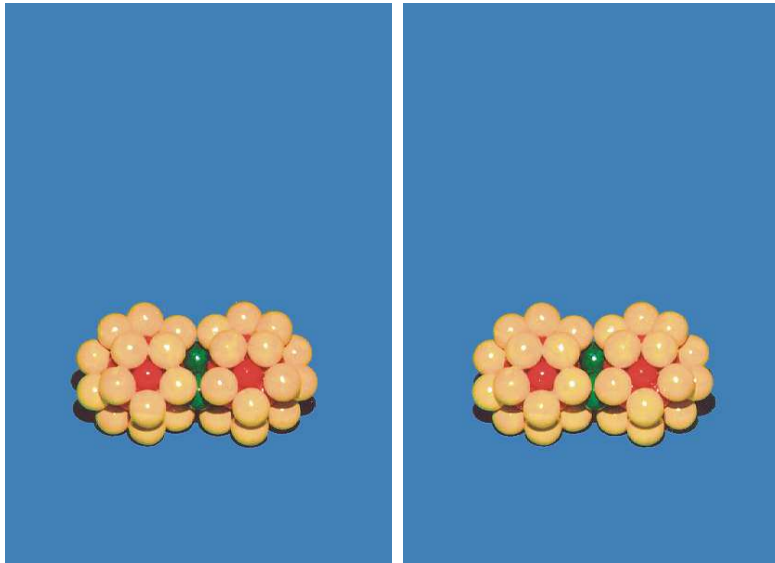


Figure 18: Two T2-clusters{1} with a common 2-fold axis and two coincidence spheres (green).

An cluster{3} has one ik-cluster{2} in the center (first shell) , 12 in the second shell, 42 in the third shell, 72 in the fourth shell etc. (a Mackay-cluster{3} with  $n$  shells;  $n < \infty$ ). A T\*1-cluster{3} has T'1-clusters{2} in the shells with an unpaired index and the T'2-clusters{2} are in the shells with a paired index, and for a T\*2-cluster{3} it is vice versa.

Nearest neighbor ik-clusters{2} from the same shell of an ik-cluster{3} have a common 2-fold symmetry axis and two coincidence ik-clusters{1}. Four or two spheres respectively of these coincidence clusters {1} are also coincidence places of nearest neighbor T1- or T2-clusters{1} from the third shell of the nearest neighbor T'1- or T'2-clusters{2}.

The position of coincidence ik-clusters{1} in the ik-clusters{2} is illustrated in **Figure 19**. The ik-clusters{1} in **Figure 19** are constructed analogously to the T'1- and T'2-cluster{2}. The three ik-clusters in the foreground have a common 2-fold axis and two coincidence places (red spheres) with their nearest neighbor ik-clusters{1}.

Nearest neighbor ik-clusters{2} from nearest neighbor shells of an ik-cluster{3} have a common 5-fold symmetry axis and 50 coincidence spheres. Each of 5 of the ik-clusters{1} from the fourth shell of an ik-cluster{2} has a common 5-fold symmetry axis and 5 coincidence spheres with each of two nearest neighbor ik-clusters{1} from the fourth shell of the nearest neighbor ik-cluster{2} and four or two of these coincidence places for spheres, respectively, are also coincidence places with a nearest neighbor ik-cluster{1} from the third shell of the nearest neighbor ik-cluster{2} from a nearest neighbor shell of an ik-cluster{3}.

**Figure 20** illustrates 20 T2-clusters{1} from the fourth shell of a T'1-cluster{2}, which is in the center of a T\*1-cluster{3}, and 30 T1-clusters{1} which belong to the fourth shell of the 12 T'2-clusters{2} that are located in the second shell of a T\*1-cluster{3}. Each of the 30 T1-

clusters{1} belongs to two T'2-clusters{2}. For a T\*2-cluster{3} it is vice versa, as can be seen in **Figure 21**. Spheres from the outer shell of T2-clusters{1} that are not on coincidence places and the spheres from the inner shells of the T1-cluster{1} are removed from the models in **Figure 20 and 21** in order to facilitate the model construction. The bigger spheres are yellow and the smaller spheres are red.

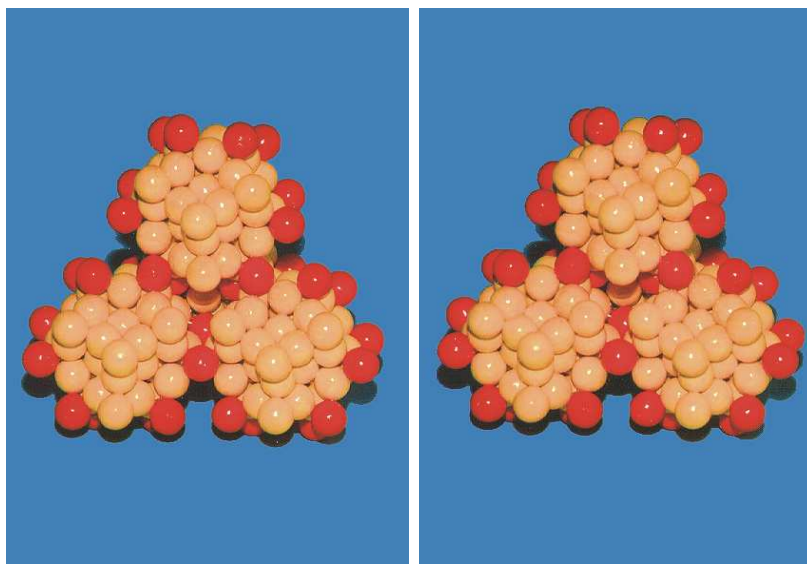


Figure 19: The ik-clusters{1} shown in this figure are constructed analogously to the T'1- and T'2-cluster{2}. The three ik-clusters{1} in the foreground have a common 2-fold axis and two coincidence places (red spheres) with their nearest neighbors.

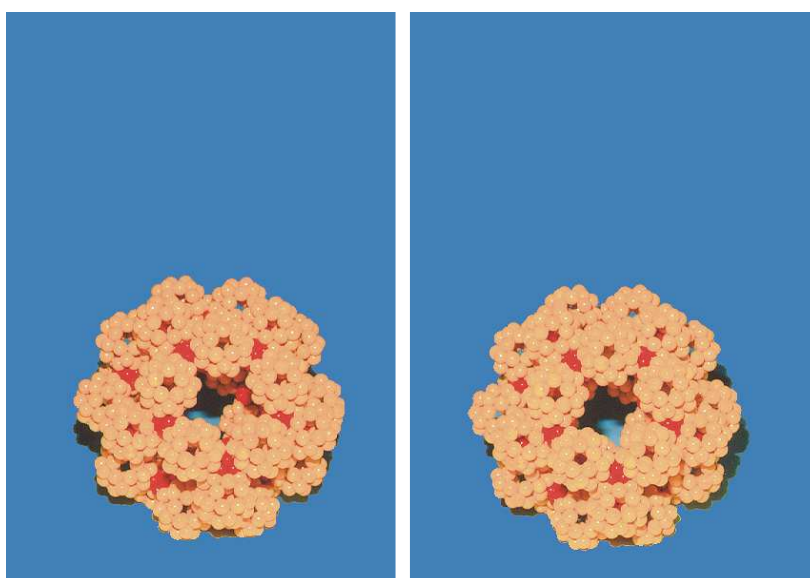


Figure 20: Part of a type T\*1-cluster {3}; see text.

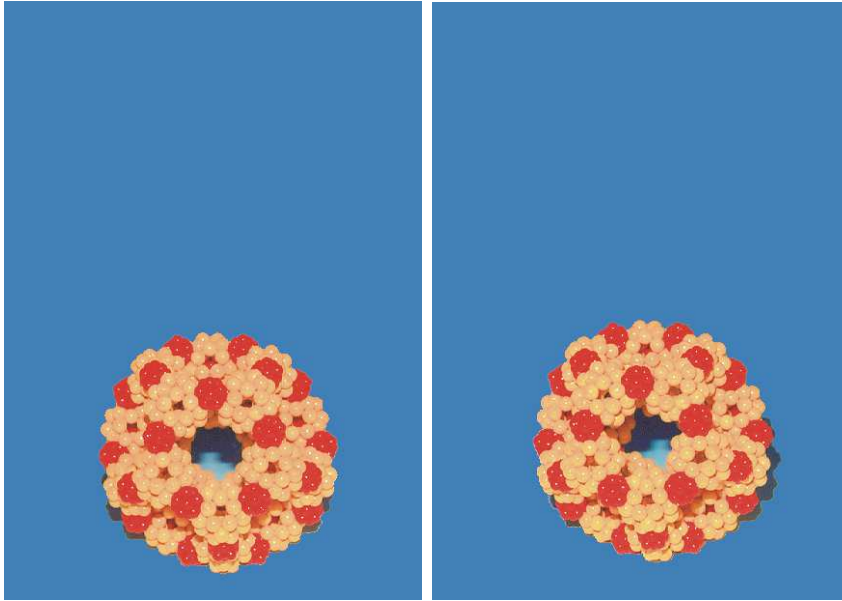


Figure 21: Part of a type T\*2-cluster {3}; see text.

Nearest neighbor single crystals of an ik-cluster{3} have a coincidence grain-boundary formed by T'1- and T'2-clusters{2}. This can be illustrated when the spheres of the ik-clusters{1} (Mackay) in **Figure 1** are replaced by the T'1- and T'2-clusters{2} in order to form a T\*1- or T\*2-cluster{3}, respectively.

The interstitial sites between ik-clusters{1} in T'1-type and T'2-type cluster{2} with  $n$  shells ( $n < \infty$ ) can be filled with one sphere each, as illustrated in **Figure 22** for a T'1-cluster{2}. Three growth stages of a T'1-cluster{2} can be seen. The yellow spheres fill the interstitial sites. In these ik-clusters{2} the space is completely filled with a dense packing of spheres.

In a T\*1-cluster{3} and a T\*2-cluster{3}, the interstitial space between T1;2-clusters{2} can be filled with ik-clusters{1} and additional spheres, as described in reference [2]. These interstitial spaces can be partly fill by completion of the 3<sup>rd</sup> shell of the T'1- and T'2-clusters{2} with “slightly retarded growing” T1- and T2-clusters{1} on the 5-f axes of the T'1- and T'2-clusters{2}; e.g. one sphere of the 3<sup>rd</sup> shell of T1-clusters{1} on the third shell of a T'1-cluster{2} (on a 2-fold axis of the T'1-cluster{2}) interferes with the formation of a nearest neighbor T1-cluster{1} on the 3<sup>rd</sup> shell of a T'1-cluster{2} (on a 5-f axis) – see **Figure 12**. The same kind of space can be filled always in the same way.

The rhombohedral unit cell of this i-prototype approximant structure contains about 12'500 spheres [2]. When the bigger spheres in the same shell of the ik-clusters{1} touch nearest neighbors and their diameter is  $d = 1$  [a.u.] the parameters of the unit cell are  $a = b = c = 21.1$  [a.u.] and  $\alpha = \beta = \gamma = 63.43^\circ$ .

**Figure 23** shows on the left side a rhombohedron containing 27 spheres (14 red ones and 13 yellow ones) and on the right side a rhombohedron containing 8 spheres. If, for example, the yellow spheres are replaced by T'1-clusters{2} and the red spheres by T'2-clusters{2}, then the center of T'1-clusters{2} and T'2-clusters{2} at the edges and in the corners of the

rhombohedrons are also on the edge of the unit cell (left side) and the sub unit cell (right side) of the i-prototype approximant structure. A unit cell contains 8 sub-unit cells with two different orientations.

Two different unit cells (13 red spheres and 14 yellow spheres or vice versa) describe the same structure.

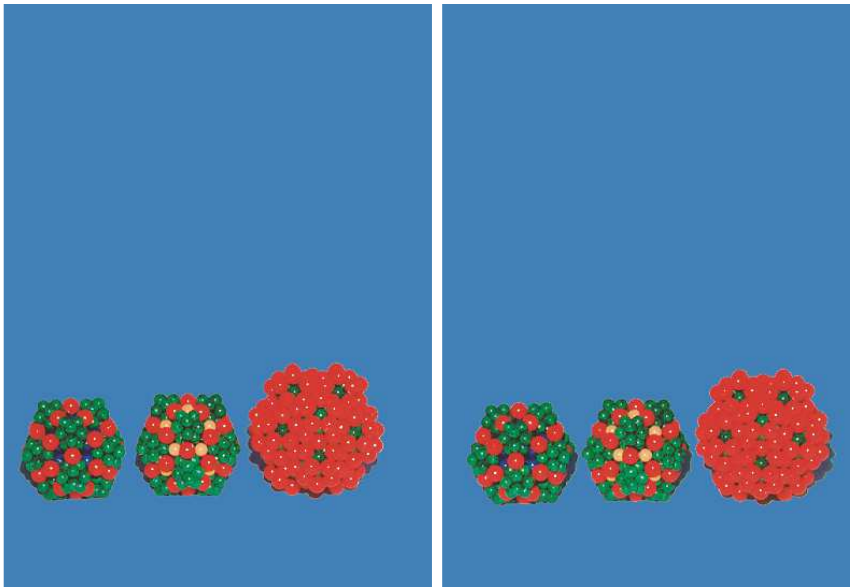


Figure 22: Three intermediate states of the growth of a  $T' 1\text{-cluster}\{2\}$ . The yellow spheres fill the interstitial sites between  $ik\text{-clusters}\{1\}$ .

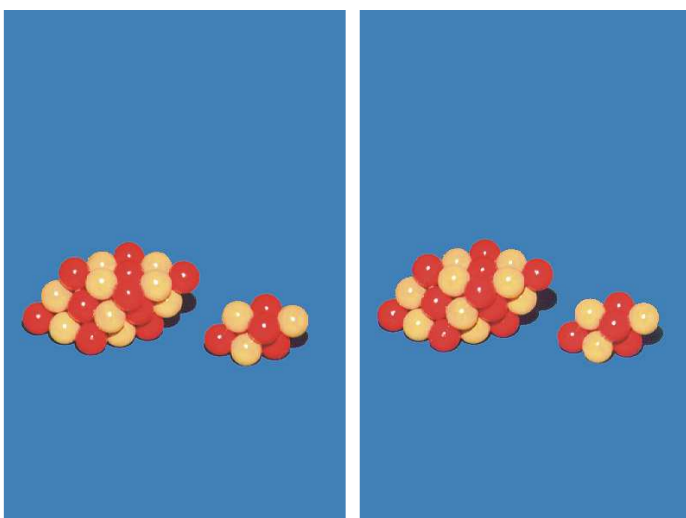


Figure 23: A rhombohedron containing 27 spheres on the left side and a rhombohedron containing 8 spheres on the right side.

### 3.1 A Model of the Atomic Structure of Icosahedral Quasicrystals

The point pattern depicted in **Figure 24** shows the projection of the centers of T1- and T2-clusters{1} of a T'1- or T'2-cluster{2}, being taken parallel to one of the 5-fold axes. The red point indicates also the projection of the center of the T'1- or T'2-cluster{2}, respectively.

The point pattern depicted in **Figure 25a** shows the projection of the centers of T1- and T2-clusters{1} from the approximant model, being taken parallel to one of the 5-fold axes of columns of The T'1;2-clusters{2}. The projection along 3 different 5-fold axes of the ik-clusters is a projection parallel to the 5-fold axis of columns of T'1;2-cluster{2}, but the projection along the other three 5-fold axes is different [2]. Red points again indicate the projection of centers of ik-clusters{2}.

**Figure 25b** illustrates the distance sequence between points from one red point to a nearest neighbor red point; it is LSLSL;  $L/S = \tau$ . If the points between two parallel nearest neighbor lines in **Figure 25a** are connected by lines which are parallel to these lines, the distance sequence between the lines is ls|sv|sl (s + v = l;  $l/s = \tau$ ;  $s/v = \tau$ ), as demonstrated in **Figure 25c**.

In the literature there are several images from i-quasicrystals taken by a high resolution transmission electron microscope (HRTEM), revealing point pattern and point-distance sequences very similar to those shown in **Figure 25a**. A section of an HRTEM image published by Hiraga [9] is nearly identical to **Figure 25a**. The arrows and pentagons are in analogous positions in both images. More examples are discussed in reference [2].

The alloy investigated by Hiraga contained aluminum, manganese and silicon. If the diameter of aluminum ( $d_{Al} = 0.2862$  nm) is introduced to the i-prototype approximant structure as the diameter of the bigger spheres, then equivalent distances between points of the two patterns differ by less than 3 % [2].

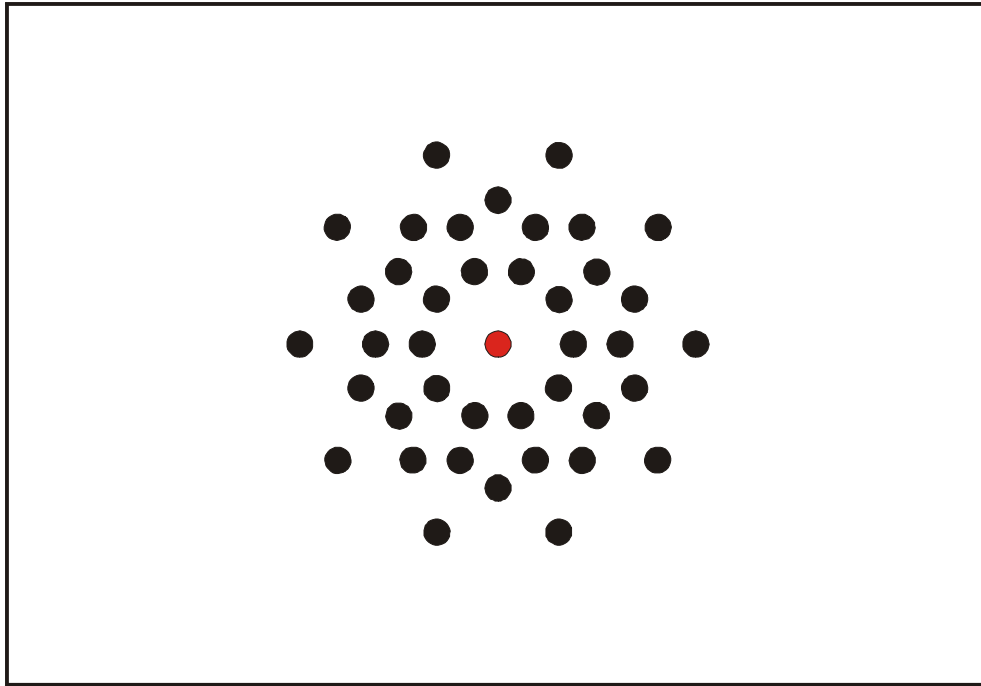


Figure 24: The projection of the center of  $T_{1;2}$ -clusters{1} of a  $T'1$ - or  $T'2$ -cluster{2}, taken parallel to one 5-fold axis. The red point indicates also the projection of the center of the  $T'1$ - or  $T'2$ -clusters{2}, respectively.

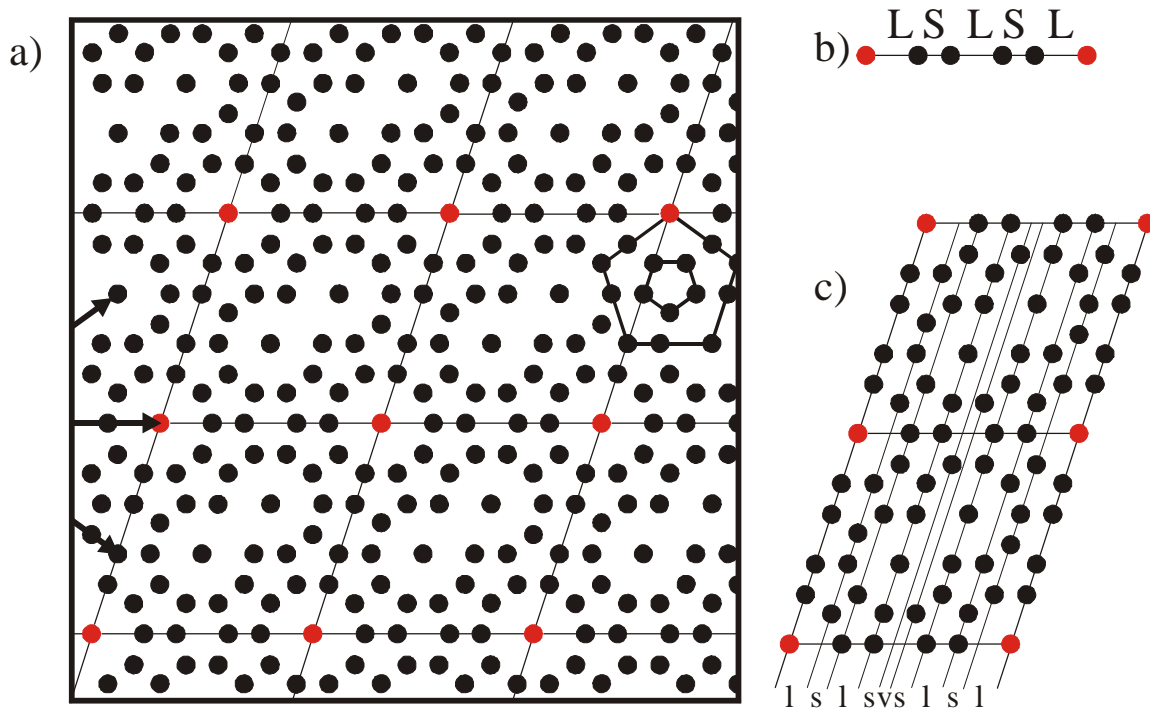


Figure 25a: The projection of the centers of  $T_{1;2}$ -clusters{1} of  $T'1$ - and  $T'2$ -clusters{2}, taken parallel to one of the 5-fold axes of the  $ik$ -clusters{1;2}, which is parallel to columns of  $ik$ -clusters{2}. The red points indicate also the projection of the centers of  $ik$ -clusters{2}.

Figure 25b: The distance sequence between the points is LSLSL; see text.

Figure 25c: The distance sequence between the parallel lines is lslsvslsl; see text.

i-quasicrystals can be seen as i-approximants (“tetrahedra of ik-cluster crystals{3}”) with phasons and other defects. The meaning of the term “phason“ in this publication differs from its use in the scientific literature. Idealized phasons in the i-prototype approximant structure described above are a layer (nearest neighbor layers) or an area of a layer (nearest neighbor layers) of incomplete  $T'1;2$ -clusters{2}. These layers are for example perpendicular to the 3-fold axis of a single quasicrystal, parallel to a 5-fold axis (three of the six) of a single quasicrystal or parallel to the plane between two 5-fold axes (three of the six). These phasons can be seen as a “layer misfit” or “layer defect”. For example, the red points on the same line in **Figure 25a** represent the positions of the 5-fold symmetry axis of columns of  $T'1;2$ -cluster{2} and together these  $T'1;2$ -cluster{2} columns represent an area of a layer of  $T'1;2$ -clusters{2}. When the distance between nearest neighbor layers of  $T'1;2$ -clusters{2} is reduced and the point distance sequence between nearest neighbor layers is, e.g., LSL, then both nearest neighbor layers have incomplete  $T'1;2$ -clusters{2} in this area.

When phasons are implemented in the i-prototype approximant structure, the periodicity can vanish completely [2]. **Figure 26 and 27** illustrate examples of phasons in the i-prototype approximant structure with a point distance sequence LS between nearest neighbor layers of incomplete  $T'1;2$ -clusters{2}. Other types of phasons are shown and discussed in reference [2].

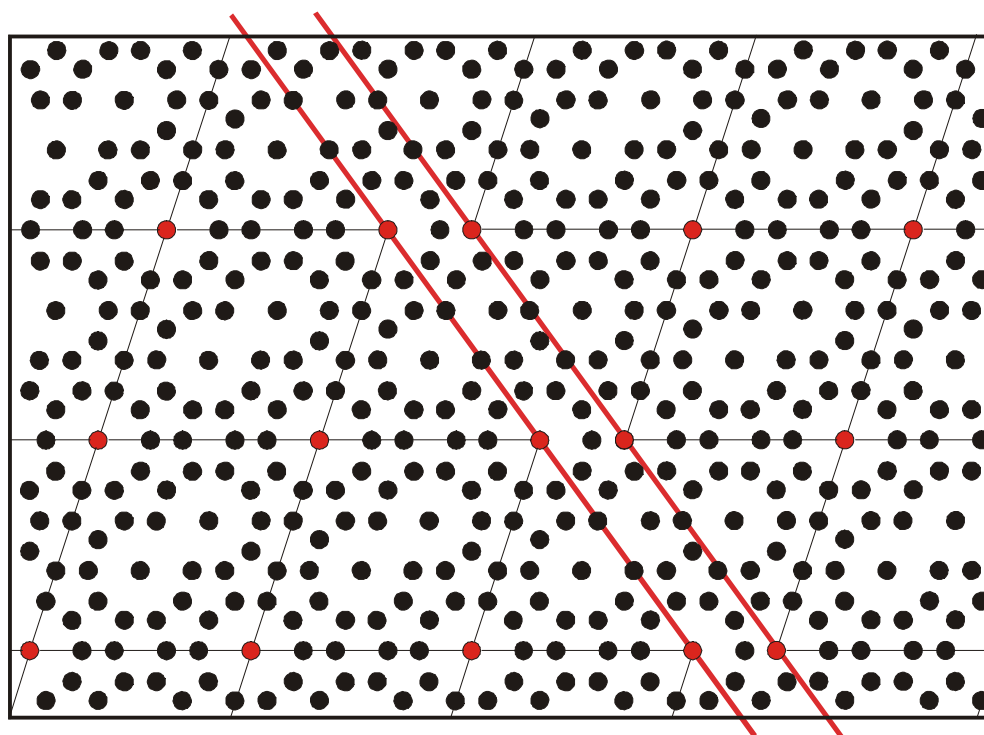


Figure 26: A phason in the i-prototype approximant structure.

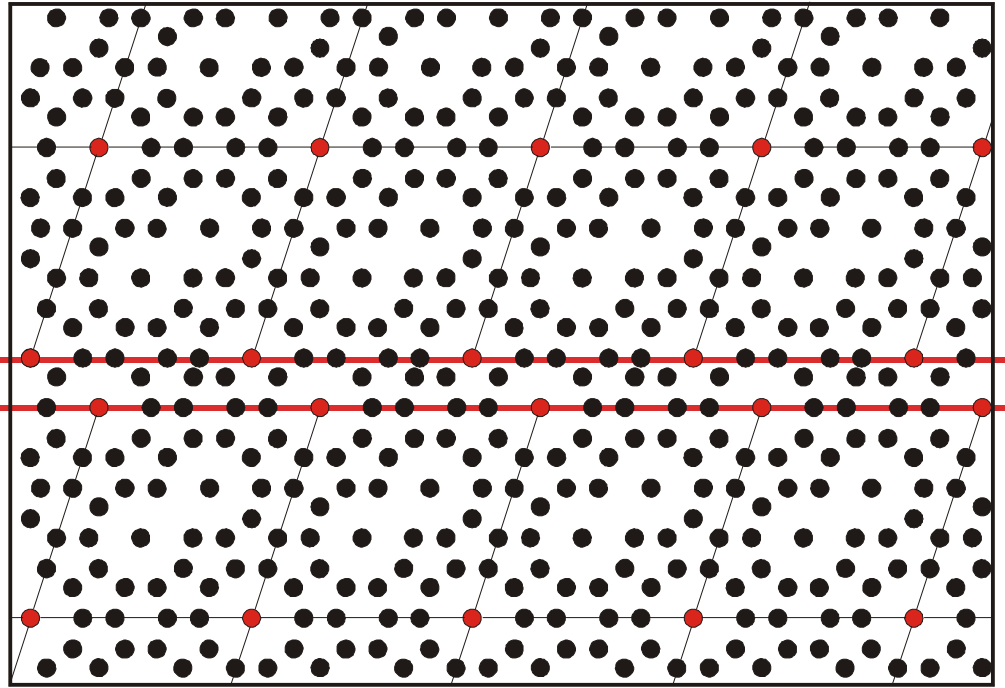


Figure 27: A phason in the i-prototype approximant structure.

The aperiodicity in a quasicrystal can also be achieved by other growth defects - by different local stress introduced by unordered point defects like vacancies or A-atoms on B-atom places or vice versa. It also has to be taken into account that nearest neighbor  $T_{1;2}$ -clusters $\{1\}$  with a common 5f-symmetry axis and 5 coincidence spheres/atoms each have one sphere/atom in the second shell that have an “overlap” with each other. This “overlap” leads to an intrinsic disorder.

Cellular automata can be described for the simulation of the solidification of  $T_{1;2}$ -clusters $\{1\}$  in i-prototype approximants and i-quasicrystals [2]. For example the corners of a cell of a  $T_{1;2}$ -Cluster $\{1\}$  can be in the centers of the spheres/atoms of the outer shell of the  $T_{1;2}$ -cluster $\{1\}$ . For i-prototype approximants, the formation of the first  $T_{1;2}$ -cluster $\{1\}$  fixes the set of all virtual cluster cells. Due to solidification, the virtual cells for  $T_{1;2}$ -clusters $\{1\}$  become “real” cells. **Figure 14 and 15** illustrate the results of four time steps of a virtual cellular automat and **Figure 20 and 21** illustrate the clusters $\{1\}$  of the 4<sup>th</sup> and the 5<sup>th</sup> time step.

For i-quasicrystals ahead of the solidification front several sets of virtual cluster cells occur. A virtual cell must have coincidence atom positions with an already solidified cell/ $T_{1;2}$ -cluster $\{1\}$ . An i-prototype approximant turns into an i-quasicrystal when  $T_{1;2}$ -clusters $\{1\}$  are the “starting cell” for an incomplete  $T_{1;2}$ -cluster $\{2\}$ , although they are not in the position of a central  $T_{1;2}$ -cluster $\{1\}$  in the center of an  $T_{1;2}$ -cluster $\{2\}$  in an i-prototype approximant.

For the simulation, the following assumption can be made: In an alloy that forms i-quasicrystals ahead of the solidification front, potential cluster positions with the most existing coincidence atom positions that are shared with already solidified atom clusters (T1;2-clusters) may occur with a higher probability than other potential atom clusters (T1;2-clusters) with less coincidence places. This may be the optimisation criterion for the formation of i-quasicrystals.

The i-prototype approximant structure has to be adjusted to the composition, the size difference of the atom species, the vacancy concentration etc. of real i-quasicrystals. Deviations from ideal compositions or ideal size differences of the components can be partly compensated by vacancies, because the vacancies can reduce local stress.

The coincidence places of nearest neighbor T1;2-clusters{1} as described in the i-prototype approximant structure lead to a kind of “directional bonding“ of nearest neighbor T1;2-clusters{1}. This is in some way analogous to the directional bonding of atoms in, e.g.,  $C_nH_m$  molecules, fullerenes or organic crystals where nearest neighbor atoms have common orbitals for electrons.

The described structure model can explain the long-range orientational order and the lack of translational symmetry in i-quasicrystals and it can explain the experimental finding of 20 single i-quasicrystals in one i-quasicrystalline grain. It is possible, to describe i-quasicrystals as cluster crystals with defects.

It is obvious that in i-quasicrystals the growth along one 3f-axis is faster than the growth along 2f-axes and 5f-axes of the ik-clusters{1;2;3}. See also section 4.1.

It should be possible to find grain boundaries in HRTEM images, that have coincidence places for T'1;2-clusters{2}. In the best case, 5 grain boundaries can be seen in the area close to a “central” 5f-axis.

A knowledge of the structure of i-quasicrystals and i-prototype approximants is of great importance, because it allows/facilitates

- the design of new i-quasicrystals with desired properties,
- an approach to the theoretical description of the electronic properties of i-quasicrystals, and an approach to find out whether quasicrystals are Hume-Rothery phases,
- a simulation of deformation processes in i-quasicrystals, and a description of dislocations – if existing – and a simulation of dislocation movement,
- a simulation of electron, neutron and X-ray diffraction of i-quasicrystals and i-prototype approximants; the i-prototype approximant (single crystal) has one 3f-axis that is different to the other nine 3f-axes and three 5f-axes that differ from the other three 5f-axes (it should already be possible to see some differences in related HRTEM images of thermodynamically stable single i-quasicrystals),
- a simulation of the influence of the structure immanent stress – a T1-clstuter{1} that shares 5 coincidence places with a T2-cluster{1} has one sphere in the inner shell (12 spheres/atoms) that “overlaps” with one sphere of the inner shell of the nearest

neighbor T2-cluster{1}, (can stress in the T1;2-clusters{1} due to the “overlap” and due to vacancies already lead to a considerable displacement of the atoms, and as a consequence of this to the absence of a crystalline diffraction pattern?) (It seems to be reasonable that the position of the atom in the center of the T1;2-clusters{1} is not occupied. The “overlap” of nearest neighbor spheres in these T1;2-clusters{1} shows, that atoms have to be given space to relax into it.) An approximant with fuzzy atom positions can be constructed and different kinds of simulations can be performed – electron diffraction, HREM imaging, etc.

- a simulation of HRTEM-images of i-quasicrystals
- a simulation of diffusion in i-quasicrystals,
- a simulation of phasons in single quasicrystals, at grainbounderies of twin single-quasicrystals, across the grainboundary of twin single-quasicrystals and a simulation of the crossing of phasons,
- a simulation of nucleation und growth of i-quasicrystals (under which conditions of which the formation of T\*1-clusters{3} is preferred against T\*2-clusters{3} and vice versa) – it may be a solidification of T1;2-clusters{1} at the solidification front rather than a solidification of single atoms. Furthermore it has to be expected, that phasons grow while the solidification front proceeds,
- a simulation of the influence of the growth in the interstitial areas between T'1;2-clusters{2} on the growth of i-quasicrystals.
- a simulation of relaxation processes in the T1;2-clusters{1} during solidification and after solidification,
- a simulation of the “mechanisms” in the T1;2-clusters{1} at the solidification front, that lead to preferred growth along the 5f-axes or the 3f-axes, respectively
- a simulation of the “mechanisms” at the solidification front, that lead to a “misplacement” of an T1;2-cluster{1} (a central T1;2-cluster{1} of a complete or partly incomplete T'1;2-cluster{2} is not in a position as it should be). A “misplacement” of a “central” T1;2-cluster{1} should induces “misplacements” of other “central” T1;2-clusters{1},
- a simulation of the relaxation of i-quasicrystals with a random distribution of point defects,
- a reasonable access to the short-range order of amorphous alloys with a similar composition,
- a simulation of decomposition in amorphous alloys,
- etc.

## 4 Models of the Atomic Structure of Decagonal Approximants

A prototype approximant structure will be described in this section and discussed in Section 4.1 in relation to the structure of decagonal quasicrystals (d-quasicrystals). A very detailed description and discussion of this model is given in reference [2].

ik-clusters{1} can be used to form ik-cluster{1} layers in the first generation with one 5-fold symmetry axis (ik-cluster{1}5f-layers{1}) and the ik-cluster{1}5f-layers{1} can be stacked to ik-cluster{1}-layer{1} columns in the first generation with one 5-fold symmetry axis (5f-columns{1}) [2]. 5f-columns{1} are the components to build 5f-columns{2}, 5f-columns{2} are the components to build 5f-columns{3} etc.

A striking feature of some of these 5f-column models is the high number of coincidence places for spheres that are shared by nearest neighbor ik-clusters{1}. Up to approximately 40% of the positions belong to two or three ik-clusters{1} equally.

A 5f-column{3} with 10 single-crystals will be briefly described and the structure of the single-crystals will be discussed as a d-prototype approximant structure being related to the structure of one type of d-quasicrystals.

The 5f-columns{1} of the 5f-column{3} have the following properties:

Five of the T2-clusters{1} (see right side of **Figure 10**) are used to form a T2-cluster{1}5f-layer{1}. Nearest neighbor T2-cluster{1} from the same T2-cluster{1}5f-layer{1} have a common 2-fold axis and 2 spheres on coincidence places (see **Figure 18**). **Figure 28** shows the A-side as the upper side of an ik-cluster{1}5f-layer{1} and **Figure 29** shows the B-side as the upper side of the same ik-cluster{1}5f-layer{1}. And  $k$  ( $2 \leq k < \infty$ ) T2-cluster{1}5f-layers{1} are put together in order to form 5f-columns{1}. **Figure 30** shows a 5f-column{1} containing 4 T2-cluster{1}5f-layers{1}. In the 5f-columns{1} an A-side of a T2-cluster{1}5f-layer{1} always meets an A-side of a nearest neighbor T2-cluster{1}5f-layer{1} and a B-side of a T2-cluster{1}5f-layer{1} always meets a B-side of a nearest neighbor T2-cluster{1}5f-layer{1}. When an A-side of a T2-cluster{1}5f-layer{1} meets the A-side of a nearest neighbor T2-cluster{1}5f-layer{1}, both layers are turned  $36^\circ$  perpendicular to their common 5-fold axis against each other and both layers share 20 coincidence spheres. When a B-side of a T2-cluster{1}5f-layer{1} meets the B-side of a nearest neighbor T2-cluster{1}5f-layer{1}, both T2-cluster{1}5f-layers{1} are not turned against each other perpendicular to the 5-fold axis and the nearest neighbor T2-cluster{1}5f-layers{1} share 25 coincidence spheres. An overlap between nearest neighbor spheres of the smaller size from different T2-clusters{1} of different T2-cluster{1}5f-layer{1} is allowed. All T2-clusters{1} in the same T2-cluster{1}5f-layer{1} have the same orientation of the symmetrical axes. Two different orientations occur in a 5f-column{1} with more than two T2-cluster{1}5f-layers{1}.

The red and blue points in **Figure 31** represent the projection of the centers of 5f-columns{2} parallel to their 5-fold axis. This figure demonstrates some properties of the 5f-column{3}

with 10 single-crystals. Nearest neighbor crystals have a common twin boundary. A central 5f-column<sub>2</sub> is surrounded by shells of 5f-columns<sub>2</sub>. The number of complete shells in **Figure 31** is  $n' = 10$ . The central 5f-column<sub>2</sub> is counted as the first shell. Nearest neighbor shells are represented by points of different color. The twin boundary of nearest neighbor single-crystals is formed by 5f-columns<sub>2</sub> which are in coincidence positions, that belong to two, three or five single-crystals, respectively. In **Figure 31** these nearest neighbor 5f-columns<sub>2</sub> on coincidence places are connected by thick lines. The 5f-column<sub>3</sub> has 5-fold symmetry and not 10-fold symmetry as it could be expected for a “decagonal” phase.

In **Figure 32** again the red and blue dots represent the projection of centers of 5f-columns<sub>2</sub> parallel to their 5-fold axis and the black points represent the projection of centers of 5f-columns<sub>1</sub> parallel to their 5-fold axis. Five 5f-columns<sub>1</sub> form a 5f-column<sub>2</sub>. It can be seen in **Figure 32** that nearest neighbor 5f-columns<sub>2</sub> of the same shell have one coincidence 5f-column<sub>1</sub> and nearest neighbor 5f-columns<sub>2</sub> from nearest neighbor shells have two coincidence 5f-columns<sub>1</sub>.

A projection parallel to the 5-fold axis of six 5f-columns<sub>2</sub> is shown in **Figure 33**. The pink and green dots are the projections of centers of ik-clusters<sub>1</sub> parallel to the 5-fold axis of the 5f-columns<sub>1;2</sub> and the black dots indicate the centers of 5f-columns<sub>1</sub>. One T2-cluster<sub>1</sub>5f-layer<sub>1</sub> is either represented by five pink or five green dots. Nearest neighbor 5f-columns<sub>1</sub> share in each T2-cluster<sub>1</sub>5f-layer<sub>1</sub> two coincidence spheres (see **Fig. 18**).

How the space within the 5f-columns<sub>1;2</sub> of the d-prototype approximant structure is filled is described in reference [2] in detail.

The rhombohedral unit cell of the d-prototype approximant structure contains about 3'600 spheres [2]. When the diameter of the bigger spheres is  $d = 1$  [a.u.] the parameters of the unit cell are  $a = b = 17.94$  [a.u.],  $c = 8.91$  [a.u.],  $\alpha = \beta = 90^\circ$ ,  $\gamma = 36^\circ$ . A set of coordinates of the spheres from the unit cell is published in reference [8]. The cross section of a unit cell, seen parallel to the 5-fold axis of the 5f-columns is illustrated in **Figure 34** by the the red lines and the enclosed area (rhombus). **Figure 34** shows an enlarged area of a single-crystal illustrated in **Figure 31**.

Several other d-prototype approximant structures are described in reference [2]; e.g.,

- the T1-cluster<sub>1</sub> described in Section 3 (left side of **Figure 10**) can be used analogously to the T2-cluster<sub>1</sub> that was used in the d-prototype approximant structure presented above.
- the 5f-columns<sub>1</sub> can be used analogously to the 5f-columns<sub>2</sub> in the d-prototype approximant structure presented above.
- a T1-cluster<sub>1</sub> can have a common 2-fold axis with each of ten nearest neighbor T1-cluster<sub>1</sub> and can share four coincidence sites for spheres with each of them. This cluster<sub>2</sub> consists of one type of spheres only.

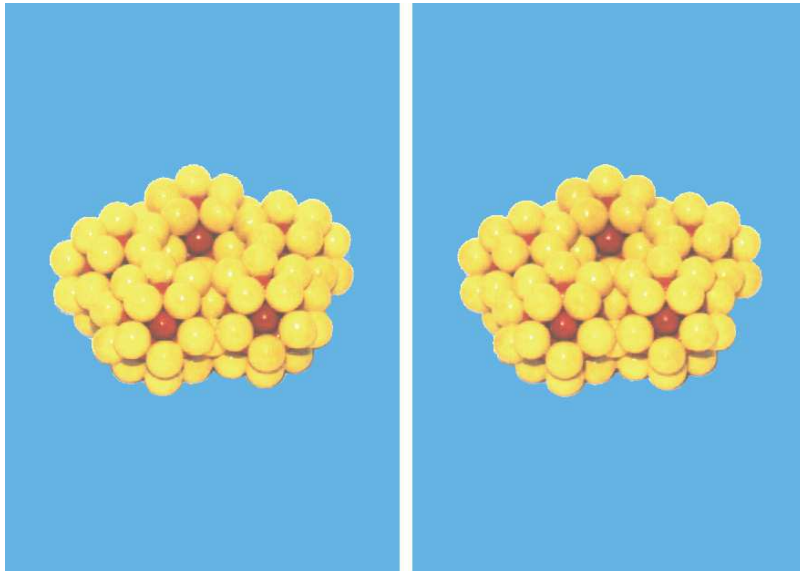


Figure 28: The A-side as the upper side of an T2-cluster{1}5f-layer{1}.

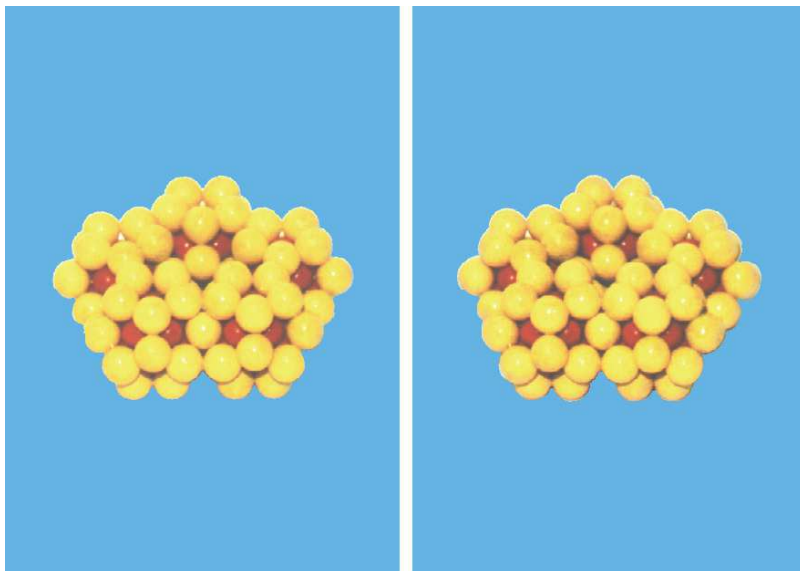


Figure 29: The B-side as the upper side of an T2-cluster{1}5f-layer{1}.

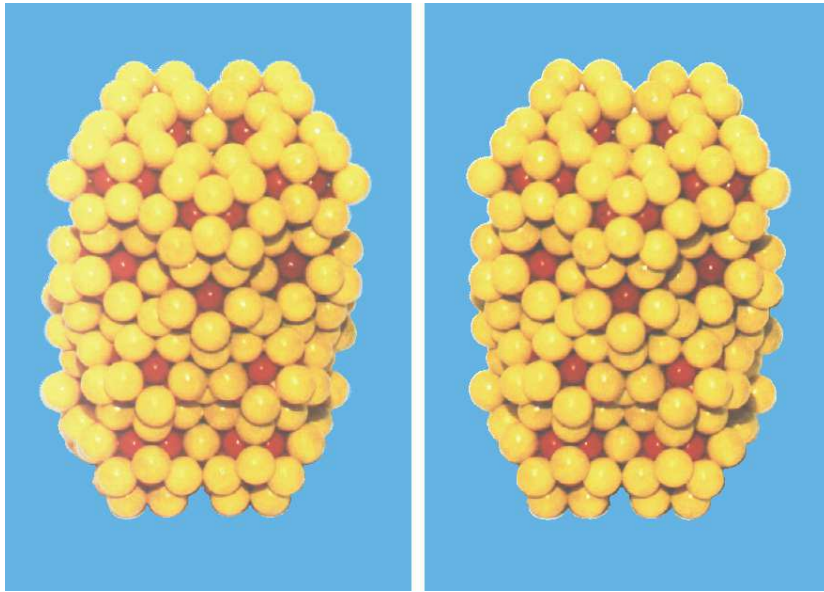


Figure 30: An 5f-column{1} containing 4 T2-cluster{1}5f-layers{1}.

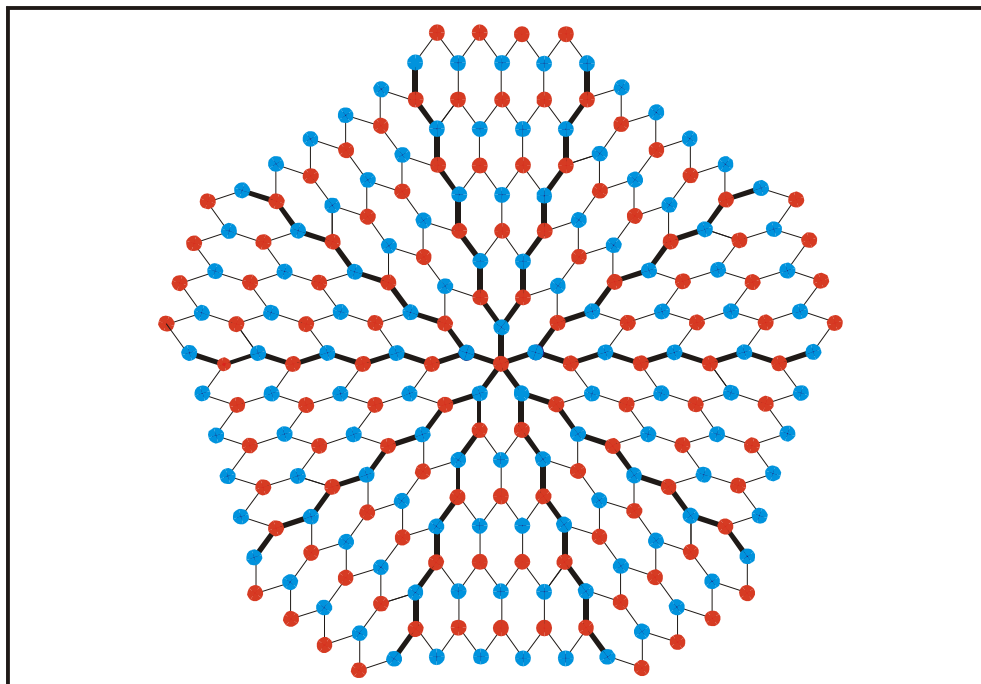


Figure 31: The red and blue dots represent the projection of the centers of 5f-columns{2} parallel to their 5-fold axis. The broad lines indicate the twin boundaries.

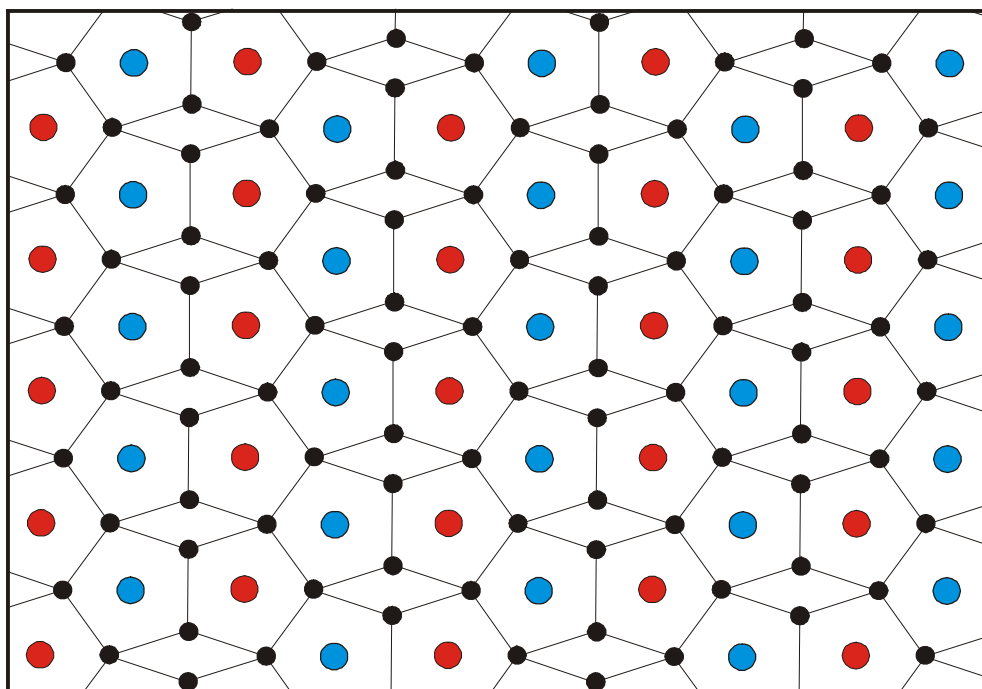


Figure 32: The red and blue dots represent the projection of centers of 5f-columns{2} parallel to their 5-fold axes and the black dots represent the projection of centers of 5f-columns{1} parallel to their 5-fold axes.

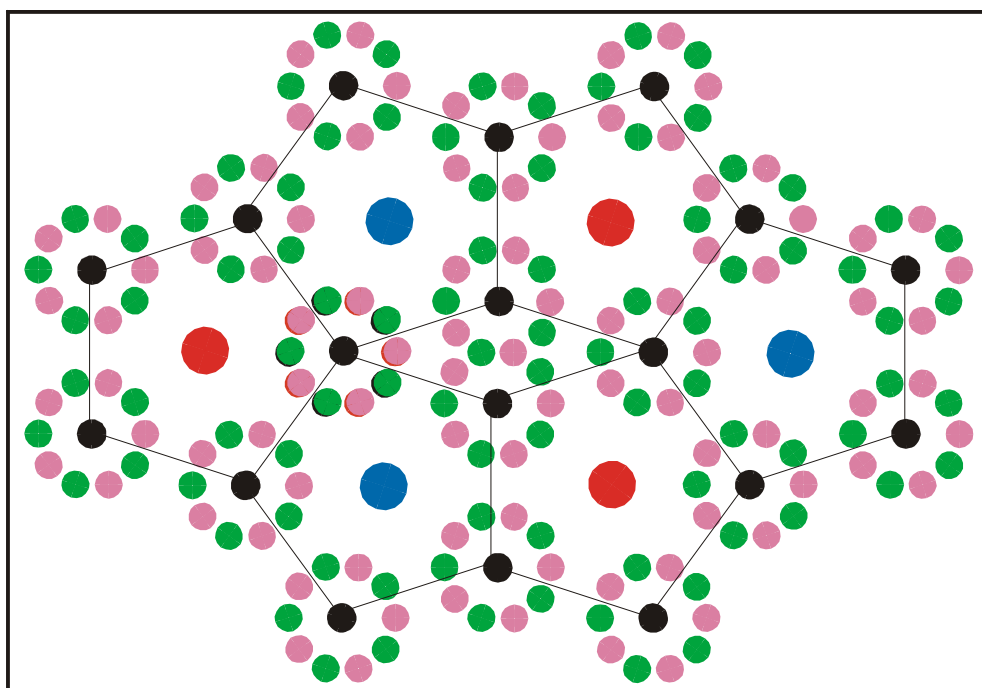


Figure 33: A projection parallel to the 5-fold axis of six 5f-columns{2}. The pink and green dots represent the projections of centers of T2-clusters{1}. One T2-cluster{1}5f-layer{1} is either represented by five pink or five green dots.

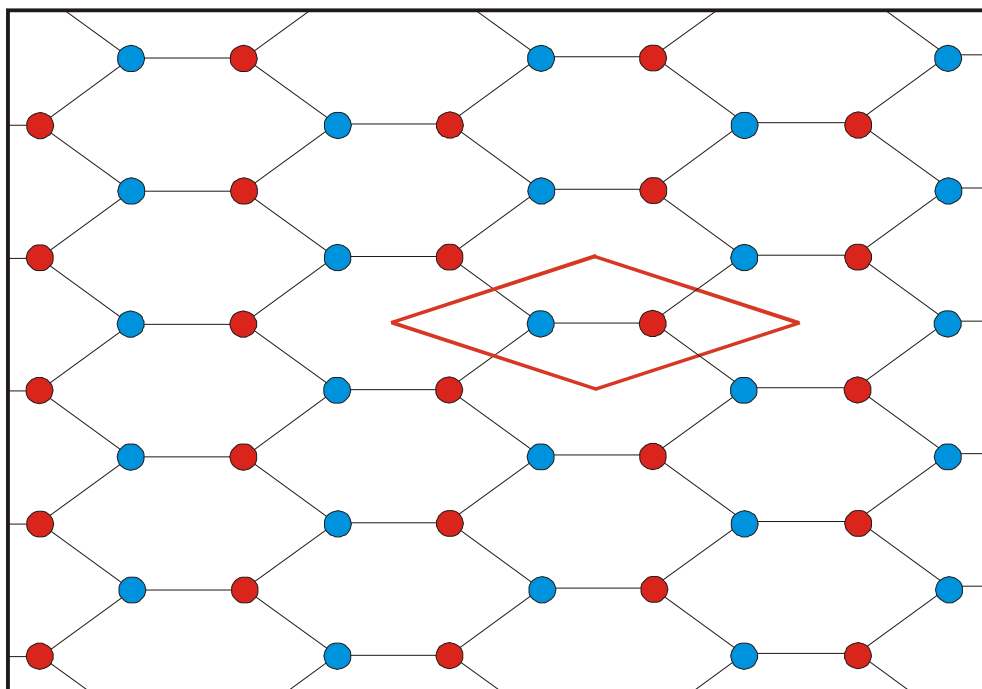


Figure 34: The red lines and the enclosed area (rhombus) illustrate the cross section of a unit cell, seen parallel to the 5-fold axis of the  $5f$ -columns{2}.

#### 4.1 Models of the Atomic Structure of Decagonal Quasicrystals

The roughly adjusted d-prototype approximant structure of AlMn or AlMnPd alloys has a rhombohedral unit cell with the parameters  $a = b = 5.13$  nm,  $c = 2.55$  nm,  $\alpha = \beta = 90^\circ$  and  $\gamma = 36^\circ$ . The diameter of the larger spheres has been replaced by the diameter of Al ( $d_{\text{Al}} = 0.2862$  nm). In the literature there are several images of d-quasicrystals taken by an HRTEM, revealing point pattern and point-distance sequences which are at least in part very similar to those shown in **Figure 33**. There is a good agreement in the size of the point pattern from the 5f-columns{1} of the adjusted d-prototype approximant structure and the analogous point pattern in an HRTEM image of a d-quasicrystalline AlMn alloy published by Hiraga [9]; the difference is less than 3%.

The point pattern of the projections of centers of ik-clusters{1} and of centers of 5f-columns{1;2} in **Figure 35** can be found as a pattern of bright dots in analogous positions in Figure 3c of reference [10]. The point pattern in one area of **Figure 35**, which is nearly identical to the one in **Figure 33** is marked by red and blue points and complete and incomplete pentagons. The alloy investigated by Beeli et al. contained Al, Mn and Pd. Analogous distances between points are 13% greater in the HRTEM image [10] than in the adjusted d-prototype approximant structure.

The periodicity of the adjusted d-prototype approximant model perpendicular to the 5f-axis is about twice the periodicity detected by Beeli et al. [10] by  $e^-$  diffraction ( $c = 1.24$  nm). But the atom layers which belong to two T1-cluster{1}5f-layers{1} turned  $36^\circ$  against each other have a periodicity of 1.27 nm. This periodicity is less than 3% greater than the periodicity detected by Beeli et al. [10].

Other adjusted prototype approximant models with a periodicity of 3.15 nm and 1.58 nm for decagonal aluminum alloys are published in reference [2]. These values are equal to or two or four times greater than published values of several different decagonal aluminum alloys, e.g., reference [11] and [12].

If phasons are implemented in the d-prototype approximant model, the periodicity can vanish completely [2]. **Figure 36 and 37** show examples of phasons in a d-prototype approximant structure.

Using cellular automata in combination with the d-prototype approximant structure might be a useful starting point for the simulation of the structure of d-quasicrystals or their nucleation and growth [2]. The d-prototype approximant structure has to be adjusted to the composition, the size difference of the atom species, the vacancy concentration etc. of real d-quasicrystals. Deviations from ideal compositions or ideal size differences of the components can be compensated by vacancies, because the vacancies can reduce local stress.

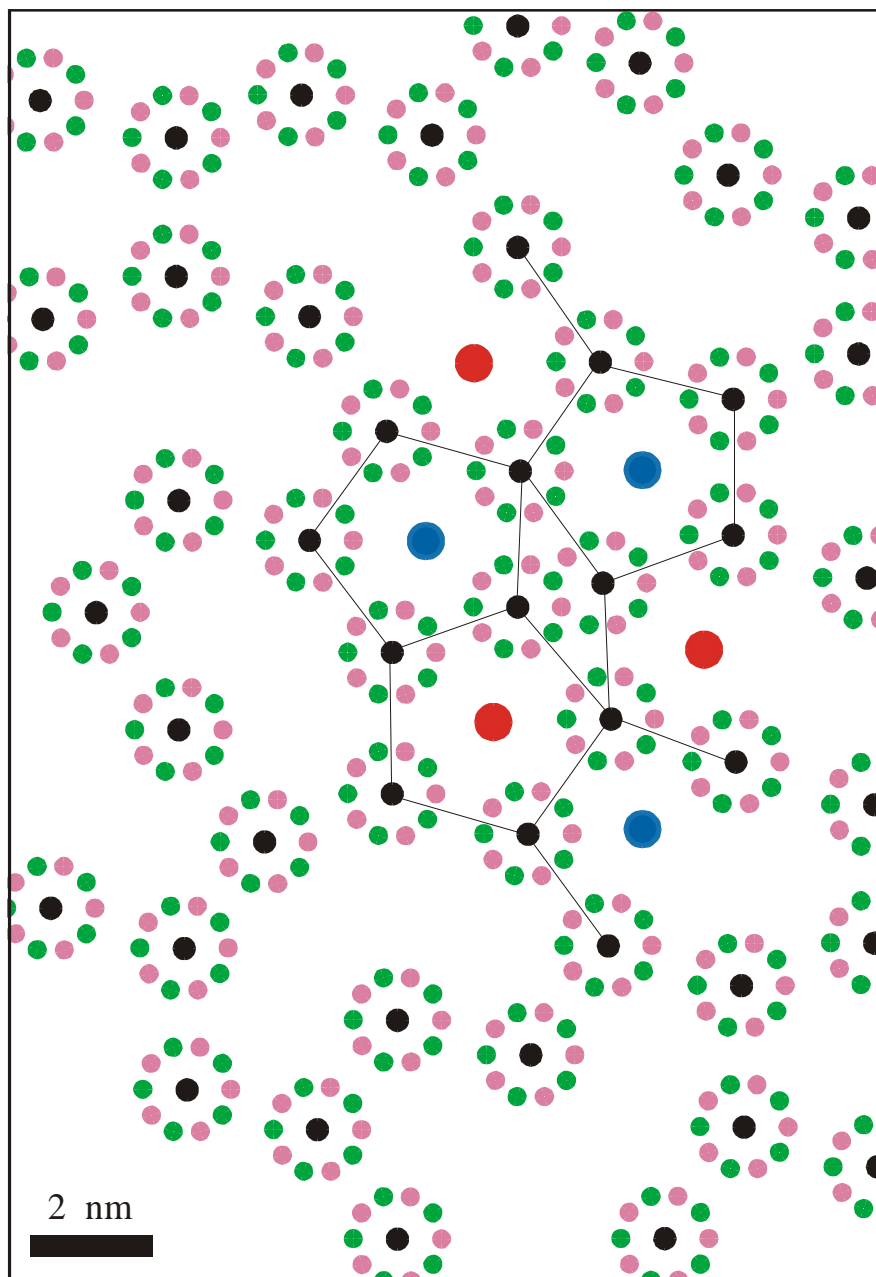


Figure 35: The point pattern of the projections of centers of T2-clusters{1} and of centers of 5f-columns{1;2} can be found as bright dots in analogous positions in Fig. 3c of reference [10]. The point pattern in one area is nearly identical to the one in Figure 33; it is marked by red and blue dots and by complete and incomplete pentagons.

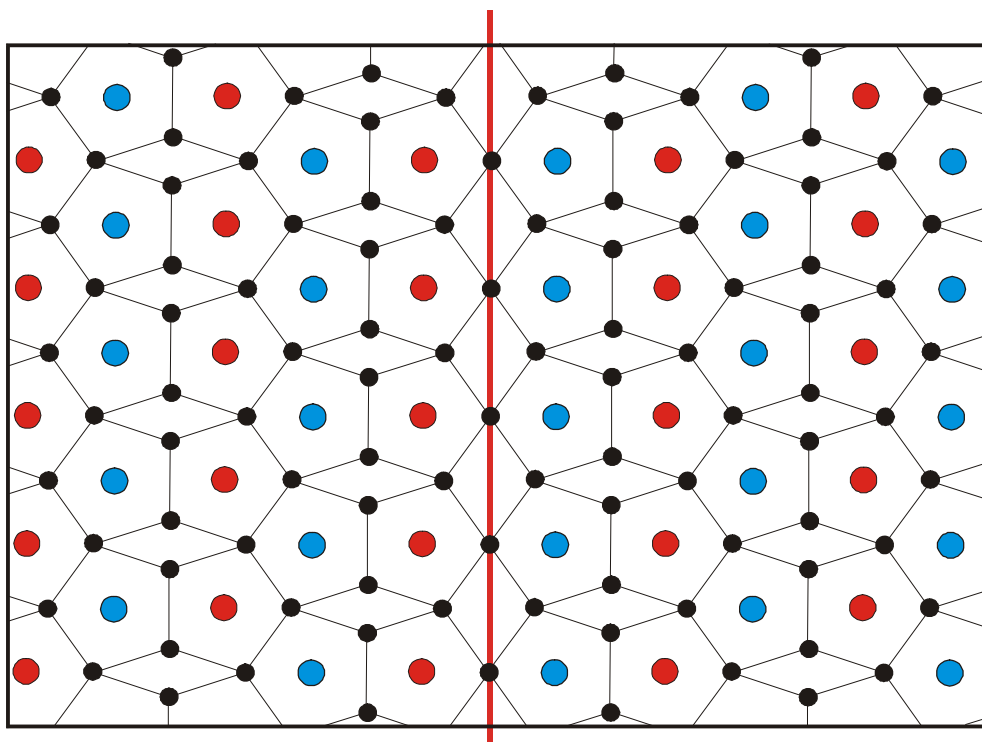


Figure 36: An example of a phason in the d-prototype approximant structure.

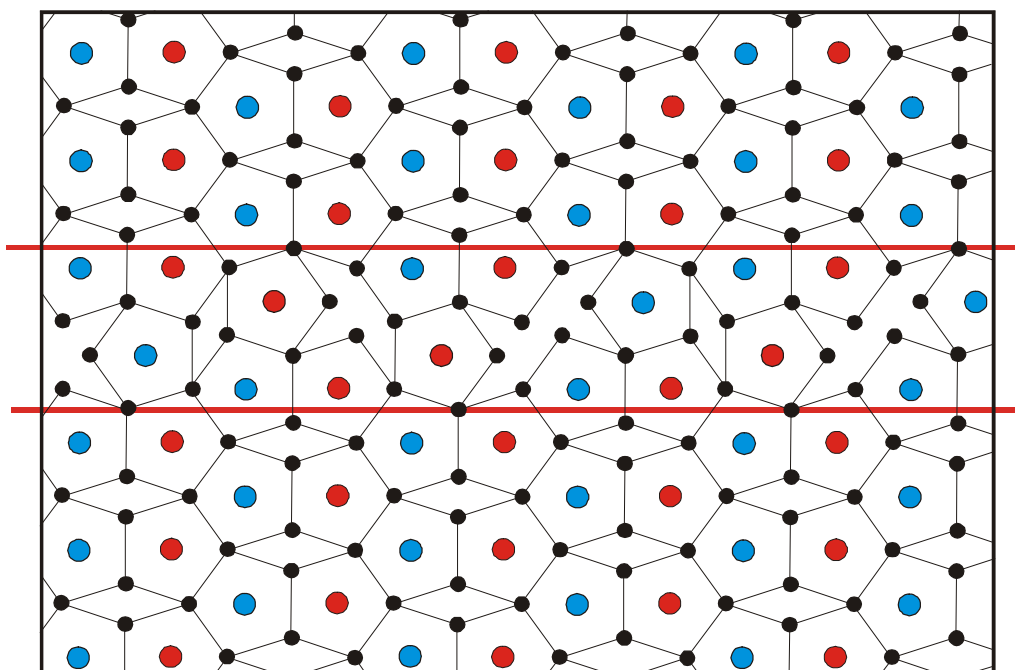


Figure 37: An example of a phason in the d-prototype approximant structure.

It should be possible to find grain boundaries in HRTEM images, that have coincidence places for 5f-columns{2}. In the best case 10 grain boundaries can be seen in the area close to the “central” 5f-axis.

It is obvious that in d-quasicrystals the growth along one 5f-axis is much faster than the growth along 2f-axes und 3f-axes of the ik-clusters{1;2}. See also section 3.1. Vacancies in the T1;2-clusters{1} on the 5-fold axis parallel to growth direction can reduce local stress.

A knowledge of the structure of d-quasicrystals is of great importance, because it allows/facilitates

- the design of new d-quasicrystals with desired attributes,
- an easier approach to the theoretical description of the electronic properties of d-quasicrystals,
- a description of dislocations in d-quasicrystals and a simulation of dislocation movement (deformation),
- a simulation of electron, neutron and X-ray diffraction of d-quasicrystals and d-prototype approximants; d-prototype approximants can be degraded step by step through growth defects and phasons,
- a simulation of the transformation from an i-quasicrystalline to a d-quasicrystalline phase [13],
- a simulation of deformation processes in d-quasicrystals, and a description of dislocations and a simulation of dislocation movement,
- a simulation of diffusion in d-quasicrystals,
- a simulation of nucleation und growth of d-quasicrystals,
- a simulation of the relaxation of d-quasicrystals with a random distribution of point defects,
- see also page 24 f.
- etc.

## Appendix

### A Nomenclature of Clusters

A nomenclature of clusters has been created in order to classify different types of clusters [3]. The general abbreviation for a cluster is: “ $mKFX^y_n$ -cluster“. “ $m$ “ stands for the cluster generation, “ $K$ “ stands for cluster, the number instead of the “ $F$ “ indicates the highest symmetry of the cluster, a “ ‘ “ or a “ ” “ after the  $F$  indicates whether it is a cluster of the type depicted in **Figure 1** or in **Figure 2** respectively, the number instead of the “ $X$ “ indicates the type of the tetrahedrons that form the cluster, the number instead of the “ $y$ “ indicates different attributes of the cluster and the number instead of the “ $n$ “ gives information about the number of completely filled shells; beginning with the first shell.

Examples:

- In **Figure 1** a single sphere, a  $^1K5'2^0_2$ -cluster, a  $^1K5'2^0_3$ -cluster and a  $^1K5'2^0_4$ -cluster can be seen.
- In **Figure 2** a  $^1K5''2^{0(+)}_1$ -cluster, a  $^1K5''2^{0(+)}_2$ -cluster, a  $^1K5''2^{0(+)}_3$ -cluster and a  $^1K5''2^{0(+)}_4$ -cluster are depicted.

For an ik-cluster{1},  $y = 0$  means that all sphere positions in the  $n$  shells are occupied and  $y = 0(+)$  means that all sphere positions in the  $n$  shells are occupied and in addition the 12 pearl positions in the  $n+1$  shell which are on the 5-fold axes are occupied.

- **Figure 5** shows a  $^1K5'2^1_2$ -cluster on the left side, a  $^2K5'2^{13}_2$  ( $^1K5'2^1_2$ )-cluster in the middle and a  $^3K5'2^{13}_2$  ( $^1K5'2^1_2$ )-cluster on the right side.

The different color of the spheres can be ignored.  $y = 1$  means that only all the positions in the  $n^{\text{th}}$  shell are occupied and nearest neighbor spheres or clusters respectively touch each other and  $y = 3$  means a cluster or a modified sphere is used to build the cluster.  $y = 13$  means a combination of  $y = 1$  and  $y = 3$ . If a cluster has several generations, then the abbreviation for the cluster with the higher generation stands before the abbreviation for the cluster with the lower generation. If the abbreviation for a cluster generation is the same as for the following generation(s), then the abbreviation for the following generation(s) is not indicated (e.g. ik-cluster{3} on the right side of **Figure 5**).

- In **Figure 7** a  ${}^2\text{K5}''2^{3(+)}_1$  ( ${}^1\text{K5}''2^1_1$ )-cluster with red spheres between the ik-clusters{1} from nearest neighbor shells is depicted on the left side and a  ${}^1\text{K5}''2^{0(+)}_1$ -cluster on the right side.

- In **Figure 8** a  ${}^2\text{K5}'2^{3(*)}_2$  ( ${}^1\text{K5}''2^1_1$ )-cluster with blue spheres between the ik-clusters{1} from nearest neighbor shells is depicted on the left side and a  ${}^1\text{K5}'2^{0(*)}_2$ -cluster on the right side. (In a  ${}^m\text{K5}'2^{3(*)}_2$ -cluster, the first and the second shell are complete, in the third shell the positions on the 5-fold axes are not occupied and in the fourth shell only the positions on the 3-fold axes are occupied.)

- The T\*1-cluster{3} of the i-prototype approximant structure:

${}^3\text{K5}'2^{34}_n$  ( ${}^2\text{K5}'2^{34(*)}_2$  ( ${}^1\text{K5}'2^{3(-)}_3$  /  ${}^1\text{K5}''2^{137}_1$ ) /  ${}^2\text{K5}'2^{34(*)}_2$  ( ${}^1\text{K5}''2^{137}_1$  /  ${}^1\text{K5}'2^{3(-)}_3$ ))-cluster ....

y = 4: the cluster type on the shells with an unpaired index - the first cluster in parentheses - differ from the cluster type on the shells with a paired index - the second cluster in parentheses; y = (-): in the last shell, the positions on the 5-fold axes are not occupied; y = 7: a  ${}^1\text{K5}'2^3_2$ -cluster of smaller spheres fills the space in the center of the cluster.

The information about special properties of a cluster have to be added in words; e.g.:

- coincidence places,
- how the space between clusters is filled,
- etc.

- The T\*2-cluster{3} of the i-prototype approximant structure:

${}^3\text{K5}'2^{34}_n$  ( ${}^2\text{K5}'2^{34(*)}_2$  ( ${}^1\text{K5}''2^{137}_1$  /  ${}^1\text{K5}'2^{3(-)}_3$ ) /  ${}^2\text{K5}'2^{34(*)}_2$  ( ${}^1\text{K5}'2^{3(-)}_3$  /  ${}^1\text{K5}''2^{137}_1$ ))-cluster ....

Clusters from different generations in one ik-cluster of the  $m^{\text{th}}$  generation can have a different abbreviation in each generation. E.g., the “y“ and/or the “n“ can be different in each generation. It is also possible that ik-clusters with F' and F'' occur in the same ik-cluster{m}.

More information about the nomenclature of clusters and especially of ik-clusters can be found in reference [3].

The nomenclature of sphere/cluster layers and sphere/cluster-layer columns is partly analogous to the nomenclature of ik-clusters{m} [3].

## References

- [1] D. Shechtman, I. Blech, D. Gratias und J. W. Cahn, Phys. Rev. Lett. **53** (1984) 1951
- [2] Quasikristalle - selbstähnliche Atomcluster „am Rande des Chaos“;  
Strukturmodelle für Approximanten und Quasikristalle, 4th ed., Hartwig Schlüter,  
SCHLÜTER CONSULT, Göttingen, to be published 2012  
(1st ed., SCHLÜTER CONSULT, 1998; 2nd ed. SCHLÜTER CONSULT, 1999;  
3rd. ed., SCHLÜTER CONSULT, 2000)
- [3] Selbstähnliche Cluster - komplexe Strukturen „am Rande des Chaos“; 2nd ed.,  
Hartwig Schlüter, SCHLÜTER CONSULT, Göttingen, to be published 2012  
(1st ed., SCHLÜTER CONSULT, 1998)
- [4] The Fractal Geometry of Nature, B. B. Mandelbrot; H. W. Freeman, San Francisco 1983
- [5] The Beauty of Fractals, H.-O. Peitgen, and P. H. Richter; Springer Verlag, Berlin 1986
- [6] Fractals, Chaos, Power Laws. Minutes from an Infinite Paradise, Manfred Schroeder;  
W. H. Freeman and Company, New York 1991  
Fraktale, Chaos und Selbstähnlichkeit; Notizen aus dem Paradies der Unendlichkeit,  
Manfred Schroeder, Spektrum, Akad. Verlag, Heidelberg 1994
- [7] A.-L. Mackay; Acta Cryst. **15** (1962) 916
- [8] M. Audier, and P. Guyot (1990) in Quasicrystals and incommensurate structures  
in condensed matter. Third International Meeting on Quasicrystals, Mexico, May  
1989 (ed. M.J. Yacaman, D. Romeu, V. Castano, and A. Gomez) pp. 288-299.  
World Scientific, Singapore.
- [9] K. Hiraga, JEOL news, Vol. 25E, No.1, (1987) 8
- [10] C. Beeli, H.-U. Nissen, and J. Robadey, Phil. Mag. Lett., **63** (1991) 87
- [11] L. Ma, R. Wang, and K. H. Kuo Scripta Met. 22, (1988) 1791
- [12] L. X. He, Y. K. Wu, and K. H. Kuo, J. Mater. Sci. 7 (1988) 1284
- [13] R. J. Schaefer, and L. Bendersky, Scripta Met. **20** (1986) 745